

# **First Search for Heavy Neutral Leptons with IceCube DeepCore**

**Dissertation**  
zur Erlangung des akademischen Grades  
doctor rerum naturalium  
(Dr. rer. nat.)

im Fach: Physik  
Spezialisierung: Experimentalphysik

eingereicht an der  
Mathematisch-Naturwissenschaftlichen Fakultät  
der Humboldt-Universität zu Berlin

von  
**Leander Fischer M. Sc.**  
geboren am 24. Oktober 1992  
in Heidelberg

Präsidentin der Humboldt-Universität zu Berlin  
Prof. Dr. Julia von Blumenthal

Dekanin der Mathematisch-Naturwissenschaftlichen Fakultät  
Prof. Dr. Caren Tischendorf

### **Copyright Notice**

This book is released into the public domain using the CC-BY-4.0 code.

To view a copy of the CC-BY-4.0 code, visit:

<https://creativecommons.org/licenses/by/4.0/>

### **Colophon**

This document was typeset with the help of KOMA-Script and L<sup>A</sup>T<sub>E</sub>X using the open-source kaobook template class.

The source code of this thesis is available at:

[https://github.com/LeanderFischer/phd\\_thesis](https://github.com/LeanderFischer/phd_thesis)

# Abstract

The observation of neutrino oscillations has established that neutrinos have non-zero masses. This phenomenon is not explained by the standard model of particle physics, but a viable explanation to this dilemma is the existence of heavy neutral leptons, which are right-handed neutrinos with masses much larger than the observed neutrino masses ( $\gg$ eV).

This work presents the first search for heavy neutral leptons with the IceCube Neutrino Observatory. The standard three flavor neutrino model is extended by adding a fourth heavy mass state and allowing mixing with the tau neutrino through the mixing parameter  $|U_{\tau 4}|^2$ . The strength of this mixing is tested using atmospheric neutrinos as a source flux. Muon neutrinos that oscillated into tau neutrinos can produce heavy neutral leptons through neutral current interactions, which then decay back to standard model particles. Both production and decay may produce observable light in the detector, leading to a unique signature of two cascades at low energies.

The measurement is performed through a binned, maximum likelihood fit, comparing the observed data to the expected events from atmospheric neutrinos and heavy neutral leptons. Three mass values  $m_4$  of 0.3 GeV, 0.6 GeV, and 1.0 GeV are tested using ten years of data, taken between 2011 and 2021. The fits constrain the mixing parameter to  $|U_{\tau 4}|^2 < 0.09$  ( $m_4 = 0.3$  GeV),  $|U_{\tau 4}|^2 < 0.21$  ( $m_4 = 0.6$  GeV), and  $|U_{\tau 4}|^2 < 0.24$  ( $m_4 = 1.0$  GeV) at 68% confidence level. No significant signal of heavy neutral leptons is observed for any of the tested masses, and the best fit mixing values obtained are consistent with the null hypothesis of no mixing.

Additionally, a thorough investigation of the unique low energy double cascade signature of HNLs in IceCube is performed. A benchmark reconstruction performance is estimated using a well established IceCube reconstruction tool, after optimizing it for low energy double cascade events. The limitations of the detector to observe these events are identified and their origins are discussed. This lays the fundamental groundwork for future searches for heavy neutral leptons in IceCube.

# **Zusammenfassung**

Zusammenfassung ...

# Foreword

## Editorial remarks:

- ▶ Acronyms are introduced in *italic font* the first time they are mentioned and will be used in normal font from then on.
- ▶ Software packages will be introduced in small cap font and later used in normal font.
- ▶ All references are listed in its full extent in the bibliography, but additionally, a selection (but not necessarily all) of them will be highlighted in the margin next to where they appear to smoothen the flow of reading.

## Work related (what is my original work):

- ▶ developed a method to treat detector uncertainty effects in close collaboration with former colleague (A. Trettin) which is well documented in a published paper and her thesis , but will be introduced in Section 3.2.3 and used in the main analysis of this work
- ▶ the model independent simulation chain described in Section ?? was developed exclusively by myself
- ▶ for the model dependent generator presented in Section ??, the skeletal structure was constructed by collaborators, before I took over and implemented the full model dependent simulation chain, including the correct decay widths calculations, custom cross-section, and the weighting scheme, continuously optimizing and testing it, before producing and processing the full samples for the main analysis
- ▶ say something about my PISA contribution
- ▶ both the study on how well IceCube can detect low energy double cascades in Chapter ?? and the main analysis in Chapter ?? were developed and performed by myself independently and are original work



# Todo list

Write introduction (RED) . . . . .	1
highlight a few more neutrino related open questions, to circle back to related to the HNL searches maybe? (YELLOW) . . . . .	6
add Majorana condition and mention what this means for interactions (LNV of 2) (ORANGE) . . . . .	7
Discuss lepton number conservation (pure dirac) and lepton number violation (dirac+majorana) (ORANGE) . . . . .	7
elaborate on Leptogenesis in $\nu$ MSM and sterile neutrino DM, or link some papers? (ORANGE) . . . . .	8
I think here I'd want the extended leptonic EW lagrangien, so I can explain the mass mixing and the interactions it opens up (RED) . . . . .	8
mention KENU, Belle, L3 in the text and add references (RED) . . . . .	9
mention PSI, LSND, BNL, NA3 in the text and add references (RED) . . . . .	10
mention the Z boson decay results from DELPHI (because they are strong in Utau4, too (RED)) . . . . .	10
Say something about atmospheric neutrino flux uncertainties, based on recent JP/Anatoli papers. (YELLOW) . . . . .	14
say something about matter effect? (ORANGE) . . . . .	15
say something about mass ordering? (ORANGE) . . . . .	15
Add fractions of the different particle types in the bins for benchmark mass/mixing (another table?) (ORANGE) . . . . .	22
add bin-wise pulls and pull distribution for selection of sets and rest to backup (RED) . . . . .	26
Need cite here! (RED) . . . . .	26
I could add some final level effects of some systematics on the 3D binning and maybe discuss how they are different from the signal shape, or so? (ORANGE) . . . . .	27
FInd first occurrence of "Asimov" and add reference and explain it there (RED) . . . . .	28
Add 3D BFP-data pull distribution for one mass (they look the same, no?) (RED) . . . . .	29
specify which they are, once I have them (RED) . . . . .	29
add 1-d data/mc agreement for example mass sample (0.6?) and all 3 analysis variables (RED) . . . . .	29
add table with reduced chi2 for all 1-d distributions (RED) . . . . .	29
Cite (again)! (RED) . . . . .	29
Show best fit hole ice angular acceptance compared to nominal and flasher/in-situ fits, maybe? (YELLOW)	29
Compare here the best fit oscillation parameters to the FLERCNN results and try to quantify it, stating the pitfalls of the comparitions (statistically fully dependent) (RED) . . . . .	31
make summary plot (masses and mixing limits on one) and then discuss wrt to other experiments? (RED)	31
Write conclusion (RED) . . . . .	33
Re-make plot with x,y for horizontal set one plot! . . . . .	37
Re-make plot with x, y, z for both cascades in one. . . . .	37

Re-arrange plots in a more sensible way. . . . .	37
fix design + significant digits to show (ORANGE) . . . . .	39
maybe show range/prior and then deviation in sigma, or absolute for the ones without prior . . . . .	39

# Contents

<b>Abstract</b>	iii
<b>Contents</b>	ix
<b>1 Introduction</b>	<b>1</b>
<b>2 Standard Model Neutrinos and Beyond</b>	<b>3</b>
2.1 The Standard Model . . . . .	3
2.1.1 Fundamental Fields . . . . .	3
2.1.2 Electroweak Symmetry Breaking . . . . .	4
2.1.3 Fermion Masses . . . . .	5
2.1.4 Leptonic Weak Interactions after Symmetry Breaking . . . . .	5
2.2 Beyond the Standard Model . . . . .	5
2.2.1 Mass Mechanisms . . . . .	6
2.2.2 Minimal Extensions and the $\nu$ MSM . . . . .	7
2.2.3 Observational Avenues for Right-Handed Neutrinos . . . . .	8
2.3 Atmospheric Neutrinos as Source of Heavy Neutral Leptons . . . . .	13
2.3.1 Production of Neutrinos in the Atmosphere . . . . .	13
2.3.2 Neutrino Oscillations . . . . .	14
2.3.3 Neutrino Interactions with Nuclei . . . . .	16
2.3.4 Heavy Neutral Lepton Production and Decay . . . . .	17
<b>3 Search for Tau Neutrino Induced Heavy Neutral Lepton Events</b>	<b>21</b>
3.1 Final Level Sample . . . . .	21
3.1.1 Expected Rates/Events . . . . .	21
3.1.2 Analysis Binning . . . . .	22
3.2 Statistical Analysis . . . . .	24
3.2.1 Test Statistic . . . . .	24
3.2.2 Physics Parameters . . . . .	25
3.2.3 Nuisance Parameters . . . . .	25
3.2.4 Low Energy Analysis Framework . . . . .	27
3.3 Analysis Checks . . . . .	27
3.3.1 Minimization Robustness . . . . .	28
3.3.2 Goodness of Fit . . . . .	28
3.3.3 Data/MC Agreement . . . . .	29
3.4 Results . . . . .	29
3.4.1 Best Fit Nuisance Parameters . . . . .	29
3.4.2 Best Fit Parameters and Limits . . . . .	30
3.4.3 Agreement with Standard Model Three-Flavor Oscillation Measurement . . . . .	31
3.4.4 Comparison to Other Experiments . . . . .	31
3.5 Outlook . . . . .	31
3.5.1 Shape Analysis Improvements . . . . .	31
3.5.2 Test Coupling to Electron/Muon Flavor . . . . .	32
3.5.3 Test Additional Coupling Processes . . . . .	32
3.5.4 IceCube Upgrade . . . . .	32
<b>4 Conclusion</b>	<b>33</b>

<b>APPENDIX</b>	<b>35</b>
<b>A Heavy Neutral Lepton Signal Simulation</b>	<b>37</b>
A.1 Model Independent Simulation Distributions . . . . .	37
A.2 Model Dependent Simulation Distributions . . . . .	38
<b>B Analysis Results</b>	<b>39</b>
B.1 Final Level Simulation Distributions . . . . .	39
B.2 Treatment of Detector Systematic Uncertainties . . . . .	39
B.3 Best Fit Nuisance Parameters . . . . .	39
<b>Figures</b>	<b>41</b>
<b>Tables</b>	<b>43</b>
<b>Bibliography</b>	<b>45</b>

# Introduction

# 1

Write introduction (RED)

## notes for the introduction

- ▶ observation of non-zero neutrino masses indicates likely existence of new physics beyond the standard model
- ▶ multiple SM neutral fermions (right handed) could explain the neutrino masses and their smallness
- ▶ if they are heavy enough to not be produced in oscillations, they are called heavy neutral leptons
- ▶
- ▶ In 1984 the PS191 [G. Bernardi et al., Phys. Lett. B 166, 479 (1986), G. Bernardi et al., Phys. Lett. B 203, 332 (1988)] experiment at CERN appears to have been the earliest beam dump to report HNL bounds from the direct production and decay.
- ▶

The neutrino was postulated by Wolfgang Pauli [1] in 1930 to explain the continuous energy spectrum of electrons originating from beta decay. Cowan and Reines confirmed this prediction of a light, neutral particle in 1956 when they discovered the electron neutrino using inverse beta decay [2]. Two additional neutrino flavors were found in the following years, and with the discovery of the muon neutrino in 1962 [3] and the tau neutrino in 2001 [4], the current theory of neutrinos in the standard model (SM) was established.

Although neutrinos were first believed to be massless, experimental evidence showing the existence of mixed neutrino states started to appear in the 1960s [5]. Mixing between different physical representations of neutrinos is proof for differences in their masses. The resulting phenomenon of neutrino oscillations can be incorporated into the standard model by extending it to include massive neutrinos. How massive they are and how strong is the mixing between neutrino states has to be obtained from measurement. Today there are a variety of precision oscillation experiments using solar, reactor and atmospheric neutrinos to tighten the constraints on the neutrino oscillation parameters. IceCube is one of those leading experiments probing the oscillation theory with atmospheric neutrinos.

The IceCube Neutrino Observatory [6] was constructed between 2004 and 2010 at the geographic South Pole. It is the first cubic kilometer Cherenkov neutrino detector and consists of 5160 optical sensors attached to 86 strings, drilled down to a maximum depth of  $\sim 2500$  m into the Antarctic ice. Neutrinos are detected by the Cherenkov light that is emitted by secondary particles produced in neutrino-nucleon scattering interactions in the ice. With DeepCore, a more densely instrumented sub-array of IceCube, the neutrino detection energy threshold can be lowered to approximately 5 GeV.

At these energies, the similarity in event signatures poses difficulties in identifying different neutrino flavor interactions. Muon neutrino charged-current interactions produce light tracks as opposed to charged-current interactions of electron and tau neutrinos as well as neutral-current interactions

[1]: Pauli (1978), "Dear radioactive ladies and gentlemen"

[2]: Cowan et al. (1956), "Detection of the Free Neutrino: a Confirmation"

[3]: Danby et al. (1962), "Observation of High-Energy Neutrino Reactions and the Existence of Two Kinds of Neutrinos"

[4]: Kodama et al. (2001), "Observation of tau neutrino interactions"

[5]: Davis et al. (1968), "Search for Neutrinos from the Sun"

[6]: Aartsen et al. (2017), "The IceCube Neutrino Observatory: instrumentation and online systems"

of all neutrinos that produce light cascades. The sparse instrumentation of IceCube makes it more challenging to separate track- and cascade-like events. In this thesis, a novel method to distinguish those two event types is developed. In contrast to previously used univariate separation techniques, the multivariate machine learning method applied here maximizes the use of information from the detector response. Through the use of a Gradient Tree Boosting algorithm the separation of events in track and cascade is improved. As a result of the improved separation, the uncertainty to the atmospheric neutrino oscillation parameters  $\Delta m_{32}^2$  and  $\theta_{23}$  is significantly reduced.

# Standard Model Neutrinos and Beyond

# 2

## 2.1 The Standard Model

The *Standard Model (SM)* of particle physics is a Yang-Mills theory [7] providing very accurate predictions of weak, strong, and *electromagnetic (EM)* interactions. It is a relativistic quantum field theory that relies on gauge invariance, where all matter is made up of fermions, which are divided into quarks and leptons, and bosons describe the interactions between the fermions that have to fulfil the overall symmetry of the theory. Leptons are excitations of Dirac-type fermion fields.

The initial idea of the theory is associated with the works of Weinberg [8], Glashow [9], and Salam [10], that proposed a unified description of EM and weak interactions as a theory of a spontaneously broken  $SU(2) \times U(1)$  symmetry for leptons, predicting a neutral massive vector boson  $Z^0$ , a massive charged vector boson  $W^\pm$ , and a massless photon  $\gamma$  as the gauge bosons. The Higgs mechanism [11], describing the breaking of the symmetry, predicts the existence of an additional scalar particle, the Higgs boson, giving the  $W^\pm$  and  $Z^0$  bosons their mass. The Higgs boson was discovered in 2012 at the LHC [12, 13].

Gell-Mann and Zweig proposed the quark model in 1964 [14, 15], which was completed by the discovery of non-abelian gauge theories [16] to form the  $SU(3)$  symmetry of the strong interaction called *quantum chromodynamics (QCD)*. QDC describes the interaction between quarks and gluons which completed the full picture of the SM in the mid-1970s. Together with the electroweak theory, the SM is a  $SU(3)_C \times SU(2)_L \times U(1)_Y$  local gauge symmetry, with the conserved quantities  $C$ , *color*,  $L$ , *left-handed chirality*, and  $Y$ , *weak hypercharge*.

In the following, the basic properties of the SM are described, following the derivations of [17, 18].

### 2.1.1 Fundamental Fields

Fermions in the SM are Weyl fields with either *left-handed (LH)* or *right-handed (RH)* chirality, meaning they are eigenvectors of the chirality operator  $\gamma_5$  with  $\gamma_5 \psi_{R/L} = \pm \psi_{R/L}$ . Only LH particles transform under  $SU(2)_L$ . The Higgs field is a complex scalar field, a doublet of  $SU(2)_L$ , which is responsible for the spontaneous symmetry breaking of  $SU(2)_L \times U(1)_Y$  to  $U(1)_{\text{EM}}$ . Local gauge transformations of the fields are given by

$$\psi \rightarrow e^{ig\theta^a(x)T^a} \psi , \quad (2.1)$$

where  $g$  is the coupling constant,  $\theta^a(x)$  are the parameters of the transformation, and  $T^a$  are the generators of the group, with  $a$  counting them. The number of bosons is dependent on the generators of the symmetry groups, while the strength is defined by the coupling constants. There are eight massless gluons corresponding to the generators of the  $SU(3)_C$  group. These

2.1	The Standard Model	3
2.2	Beyond the Standard Model . . . . .	5
2.3	Atmospheric Neutrinos as Source of Heavy Neutral Leptons . . . . .	13

[7]: Yang et al. (1954), "Conservation of Isotopic Spin and Isotopic Gauge Invariance"

[8]: Weinberg (1967), "A Model of Leptons"

[9]: Glashow (1961), "Partial-symmetries of weak interactions"

[11]: Higgs (1964), "Broken symmetries, massless particles and gauge fields"

[12]: Chatrchyan et al. (2012), "Observation of a New Boson at a Mass of 125 GeV with the CMS Experiment at the LHC"

[13]: Aad et al. (2012), "Observation of a new particle in the search for the Standard Model Higgs boson with the ATLAS detector at the LHC"

[14]: Gell-Mann (1964), "A Schematic Model of Baryons and Mesons"

[15]: Zweig (1964), "An  $SU(3)$  model for strong interaction symmetry and its breaking. Version 2"

[17]: Giunti et al. (2007), *Fundamentals of Neutrino Physics and Astrophysics*

[18]: Schwartz (2013), *Quantum Field Theory and the Standard Model*

mediate the strong force which conserves color charge. The  $W_1, W_2, W_3$ , and  $B$  boson fields of the  $SU(2)_L \times U(1)_Y$  group are mixed into the massive bosons through spontaneous symmetry breaking as

$$W^\pm = \frac{1}{\sqrt{2}}(W_1 \mp iW_2) \quad (2.2)$$

and

$$Z^0 = \cos \theta_W W_3 - \sin \theta_W B, \quad (2.3)$$

with  $\theta_W$  being the *Weinberg angle*. The massless photon field is given by

$$A = \sin \theta_W W_3 + \cos \theta_W B \quad (2.4)$$

and its conserved quantity is the EM charge  $Q$ , which depends on the weak hypercharge,  $Y$ , and the third component of the weak isospin,  $T_3$ , as  $Q = T_3 + Y/2$ .

	Type			$Q$
quarks	u	c	t	+2/3
	d	s	b	-1/3
leptons	$\nu_e$	$\nu_\mu$	$\nu_\tau$	0
	e	$\mu$	$\tau$	-1

**Table 2.1:** Fermions in the Standard Model. Shown are all three generations of quarks and leptons with their electric charge  $Q$ .

Fermions are divided into six quarks and six leptons. Weak, strong, and EM force act on the quarks, and they are always found in bound form as baryons or mesons. Leptons do not participate in the strong interaction and only the electrically charged leptons are massive and are effected by the EM force, while neutrinos are massless and only interact via the weak force. Each charged lepton has an associated neutrino, which it interacts with in *charged-current (CC)* weak interactions, that will be explained in more detail in Section 2.1.4. The fermions are listed in Table 2.1.

## 2.1.2 Electroweak Symmetry Breaking

To elaborate the process of spontaneous symmetry breaking through which the gauge bosons of the weak interaction acquire their masses, the Lagrangian of the Higgs field is considered as

$$\mathcal{L}_{\text{Higgs}} = (D_\mu \Phi^\dagger)(D^\mu \Phi) - \lambda \left( \Phi^\dagger \Phi - \frac{v^2}{2} \right)^2, \quad (2.5)$$

with parameters  $\lambda$  and  $v$ , where  $\lambda$  is assumed to be positive.  $\Phi$  is the Higgs doublet, which is defined as

$$\Phi = \begin{pmatrix} \Phi^+ \\ \Phi^0 \end{pmatrix}, \quad (2.6)$$

with the charged component  $\Phi^+$  and the neutral component  $\Phi^0$ . The covariant derivative is given by

$$D_\mu = \partial_\mu - ig_2 \frac{\sigma^i}{2} W_\mu^i - \frac{1}{2}ig_1 B_\mu, \quad (2.7)$$

with the Pauli matrices  $\sigma^i$  and the gauge boson fields  $W_\mu^i$  and  $B_\mu$  of the  $SU(2)_L$  and  $U(1)_Y$  groups, respectively. The coupling constants  $g_2$  and  $g_1$  are the respective coupling constants which are related to the Weinberg angle as  $\tan \theta_W = \frac{g_1}{g_2}$ . The Higgs potential has a non-zero *vacuum expectation value (vev)* at the minimum of the potential at  $\Phi^\dagger \Phi = \frac{v^2}{2}$ . Since the vacuum is electrically neutral, it can only come from a neutral component of the Higgs

doublet as

$$\Phi_{\text{vev}} = \frac{1}{\sqrt{2}} \begin{pmatrix} 0 \\ v \end{pmatrix}. \quad (2.8)$$

### 2.1.3 Fermion Masses

The mass term for charged fermions with spin-1/2 is given by

$$\mathcal{L}_{\text{Dirac}} = m(\bar{\Psi}_R \Psi_L - \bar{\Psi}_L \Psi_R), \quad (2.9)$$

composed of the product of LH and RH Weyl spinors  $\Psi_{L/R}$ . This term is not invariant under  $SU(2)_L \times U(1)_Y$  gauge transformations, but adding a Yukawa term

$$\mathcal{L}_{\text{Yukawa}} = -Y^e \bar{L}_L \Phi e_R + h.c., \quad (2.10)$$

coupling the fermion fields  $e_R$  to the Higgs field  $\Phi$ , recovers the invariance and gives the fermions their masses. Here,  $Y^e$  is the Yukawa coupling constant and  $\bar{L}_L$  is the  $SU(2)_L$  doublet. With the vev, this results in the mass term for the charged leptons and down-type quarks of  $-m_e(\bar{e}_L e_R + \bar{e}_R e_L)$  with  $m_e = \frac{Y^e v}{\sqrt{2}}$ . With  $\tilde{\Phi} = i\sigma_2 \Phi^*$ , a similar Yukawa term can be written as  $-Y^u \bar{L}_L \tilde{\Phi} u_R + h.c.$ , which leads to the masses of the up-type quarks.

### 2.1.4 Leptonic Weak Interactions after Symmetry Breaking

After the spontaneous symmetry breaking, the leptonic part of the electroweak Lagrangian can be written as

$$\begin{aligned} \mathcal{L}_{\text{EW}}^\ell &= \frac{g}{\sqrt{2}} W^+ \sum_{\alpha=e,\mu,\tau} \bar{\nu}_\alpha \gamma^\mu P_L \ell_\alpha + \frac{g}{4c_w} Z \\ &\times \left\{ \sum_{\alpha=e,\mu,\tau} \bar{\nu}_\alpha \gamma^\mu P_L \nu_\alpha + \sum_\alpha \bar{\ell}_\alpha \gamma^\mu [2s_w^2 P_R - (1 - 2s_w^2) P_L] \ell_\alpha \right\} + h.c., \end{aligned} \quad (2.11)$$

where  $c_w \equiv \cos \theta_w$ ,  $s_w \equiv \sin \theta_w$ ,  $P_L$  and  $P_R$  are the left and right projectors, respectively, while  $\nu_\alpha$  and  $\ell_\alpha$ , are the neutrino and charged lepton weak eigenstates. The  $W^\pm$  and  $Z$  bosons are the massive gauge bosons of the weak interaction. The large boson masses  $m_W \sim 80 \text{ GeV}$  and  $m_Z \sim 90 \text{ GeV}$  result in a short range of the force of about  $1 \times 10^{-18} \text{ m}$ . Interactions carried out by the  $W^\pm$  bosons are called *charged current (CC)* interactions, as they propagate a charge, therefore changing the interacting lepton to its charged/neutral counterpart. *Neutral current (NC)* interactions are those mediated by the  $Z^0$  boson, where no charge is transferred. NC interactions couple neutrinos to neutrinos and charged leptons to charged leptons, but not to each other. The Feynman diagrams for CC and NC interactions are shown in Figure 2.1.

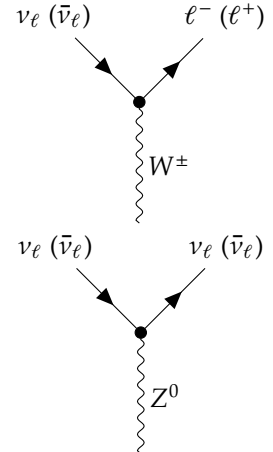


**Figure 2.1:** Feynman diagrams of charged-current (top) and neutral-current (bottom) neutrino weak interactions, modified from [19].

## 2.2 Beyond the Standard Model

The fundamentals of the SM described above are not enough to explain all observed phenomena. Gravity cannot be explained by the SM, as it is incompatible with general relativity, neither can some of the cosmological observations like *dark matter (DM)*, and the matter-antimatter asymmetry be explained. But most importantly, the SM does not predict neutrinos to

have mass, which is experimentally proven by neutrino oscillations, so some extension to the SM is needed in order to explain the observed phenomena.

[20]: Deruelle et al. (2018), *Relativity in Modern Physics*

[21]: Workman et al. (2022), “Review of Particle Physics”

[22]: Fukugita et al. (1986), “Baryogenesis without grand unification”

[5]: Davis et al. (1968), “Search for Neutrinos from the Sun”

[23]: Fukuda et al. (1998), “Evidence for Oscillation of Atmospheric Neutrinos”

[24]: Ahmad et al. (2002), “Direct Evidence for Neutrino Flavor Transformation from Neutral-Current Interactions in the Sudbury Neutrino Observatory”

[25]: Alam et al. (2021), “Completed SDSS-IV extended Baryon Oscillation Spectroscopic Survey: Cosmological implications from two decades of spectroscopic surveys at the Apache Point Observatory”

[26]: Aghanim et al. (2020), “Planck2018 results: VI. Cosmological parameters”

[27]: Aker et al. (2022), “Direct neutrino-mass measurement with sub-electronvolt sensitivity”

highlight a few more neutrino related open questions, to circle back to related to the HNL searches maybe? (YEL-LOW)

The standard cosmological model  $\Lambda$ CDM [20] assumes that equal amounts of matter and anti-matter were produced in the early universe. However, the universe today is dominantly made up of matter. This so-called *baryon asymmetry of the universe (BAU)* can be measured by the difference between the number densities of baryons and anti-baryons normalized to the number density of photons as

$$\eta_B = \frac{n_B - n_{\bar{B}}}{n_\gamma} , \quad (2.12)$$

where  $n_B$ ,  $n_{\bar{B}}$ , and  $n_\gamma$  are the number densities of baryons, anti-baryons, and photons, respectively. Baryons are the dominant component with  $\eta_B$  being observed to be at the order of  $10^{-9}$  [21]. Leptogenesis and EW baryogenesis are scenarios that could explain this phenomenon, where the former could be realized by the existence of heavy RH neutrinos [22].

The observation of neutrino flavor conversions and neutrino oscillations in a multitude of experiments [5, 23, 24] is the strongest evidence for physics *beyond the standard model (BSM)* measured in laboratories to date. The observation that neutrinos change their flavor while they propagate through space can only be explained, if at least two neutrinos have a non-zero mass. From those measurements we know the mass differences are very small as compared to the lepton masses, but neither their existence, nor their smallness is predicted by the SM. There are upper limits on the sum of all neutrino masses from cosmological observations at 1.2 eV [25, 26] and at 0.8 eV from the KATRIN experiment [27]. Adding RH neutrino states to the theory could explain the origin of the observed non-zero neutrino masses and could be tested for by searching for corresponding signatures in experiments.

## 2.2.1 Mass Mechanisms

Since there are no RH neutrinos in the SM, the mass mechanism described in Section 2.1.3, which couples the Higgs field to LH and RH Weyl fields, predicts the LH neutrinos to be massless. From experimental observations it is known that at least two of the three neutrino generations need to have a non-zero mass. Assuming the existence of RH neutrinos fields  $\nu_R$ , one way of producing the neutrino masses is by adding a Yukawa coupling term similar to the one for up-type quarks mentioned in Section 2.1.3, to write the full Yukawa Lagrangian as

$$\mathcal{L}_{\text{Yukawa}} = -Y^e_{ij} \bar{L}_L^i \Phi e_R^j - Y^\nu_{ij} \bar{L}_L^i \tilde{\Phi} \nu_R^j + h.c. , \quad (2.13)$$

with  $i, j$  running over the three generations of leptons  $e, \mu$ , and  $\tau$ , and  $Y^e$  and  $Y^\nu$  being the Yukawa coupling matrices. Diagonalizing the Yukawa coupling matrices through unitary transformations  $U^e$  and  $U^\nu$  leads to the **Dirac mass term** in the mass basis as

$$\mathcal{L}_{\text{Dirac}}^{\text{mass}} = \frac{v}{\sqrt{2}} (\bar{e}_L M_e e_R - \bar{\nu}_L M_\nu \nu_R) , \quad (2.14)$$

where  $M_e$  and  $M_\nu$  are the diagonal mass matrices of leptons and neutrinos, respectively. A purely Dirac mass term would not explain the smallness of

the neutrino masses in a straightforward way. Only fine-tuning the Yukawa coupling constants to small values would lead to small neutrino masses.

An additional way of generating neutrino masses is by adding a Majorana mass term of the form

$$\mathcal{L}_{\text{Majorana}} = -\frac{1}{2} M_{ij} (\nu_R^i)^c \nu_R^j + h.c., \quad (2.15)$$

add Majorana condition and mention what this means for interactions (LNV of 2) (ORANGE)

with  $M_{ij}$  being the Majorana mass matrix and the indices  $i, j$  running over all  $n_R$  RH neutrino generations. The superscript  $c$  denotes the charge conjugate field. Combining the charge conjugated RH neutrino fields with the LH neutrino fields as

$$N = \begin{pmatrix} \nu_L \\ \nu_R^c \end{pmatrix}, \quad (2.16)$$

with  $\nu_R$  containing the  $n_R$  RH fields. The full neutrino mass Lagrangian is then given by the combined **Dirac and Majorana mass term** as

$$\mathcal{L}_{\text{Dirac+Majorana}}^{\text{mass}, \nu} = \frac{1}{2} N^T \hat{C} M^{D+M} N + h.c., \quad (2.17)$$

and the mass matrix is given by

$$M^{D+M} = \begin{pmatrix} 0 & (M^D)^T \\ M^D & M^R \end{pmatrix}. \quad (2.18)$$

On top of explaining the origin of neutrino masses itself, a combined Dirac and Majorana mass term could also solve the question of their smallness. If the mass of the RH neutrinos is very large, the masses of the active neutrino flavors is suppressed, which is known as *see-saw mechanism*.

Discuss lepton number conservation (pure dirac) and lepton number violation (dirac+majorana) (ORANGE)

## 2.2.2 Minimal Extensions and the $\nu$ MSM

So far we have described neutrinos in their flavor eigenstates, which are relevant for weak interactions, where the three weak flavor states  $\nu_e, \nu_\mu$ , and  $\nu_\tau$  are related to the charged leptons they interact with in CC interactions. In order to *just* explain the three oscillating flavor eigenstates, three mass states are needed, which are related to the flavor eigenstates by the unitary, 3x3 *Pontecorvo-Maki-Nakagawa-Sakata* (PMNS) mixing matrix  $U$ , where the flavor states are a superposition of the mass states as

$$|\nu_\alpha\rangle = \sum_k U_{\alpha k}^* |\nu_k\rangle, \quad (2.19)$$

with the weak flavor states  $|\nu_\alpha\rangle$ ,  $\alpha = e, \mu, \tau$ , and the mass states  $|\nu_k\rangle$  with  $k = 1, 2, 3$ . In its generic form the PMNS matrix is given by

$$U = \begin{pmatrix} U_{e1} & U_{e2} & U_{e3} \\ U_{\mu 1} & U_{\mu 2} & U_{\mu 3} \\ U_{\tau 1} & U_{\tau 2} & U_{\tau 3} \end{pmatrix}, \quad (2.20)$$

which will be the basis for the discussion of neutrino oscillations in Section 2.3.2.

This however is not enough to explain the neutrino masses observed in oscillation experiments. The most minimal model required to give rise to two non-zero active neutrino masses, is an additional two RH neutrinos,

assuming the mass of the lightest SM neutrino is zero. If the additional neutrino states have masses  $\gg$ eV they are referred to as *heavy neutral leptons* (HNL), which are almost sterile, with a small mass mixing with the active neutrinos.

But the SM also fails to explain additional observations of physics beyond the standard model (BAU, DM), which could be solved by the *neutrino minimal standard model* ( $\nu$ MSM) [28, 29]. In the  $\nu$ MSM, three RH neutrinos are added, where two of them are heavy, to explain the observed neutrino masses and oscillations, and a third one is light and serves as a DM candidate. The mixing between mass and flavor eigenstates is then described by an extended 6x6 mixing matrix as

$$\begin{pmatrix} \nu_e \\ \nu_\mu \\ \nu_\tau \\ N_1 \\ N_2 \\ N_3 \end{pmatrix} = \begin{pmatrix} U_{e1} & U_{e2} & U_{e3} & U_{e4} & U_{e5} & U_{e6} \\ U_{\mu 1} & U_{\mu 2} & U_{\mu 3} & U_{\mu 4} & U_{\mu 5} & U_{\mu 6} \\ U_{\tau 1} & U_{\tau 2} & U_{\tau 3} & U_{\tau 4} & U_{\tau 5} & U_{\tau 6} \\ U_{N_1 1} & U_{N_1 2} & U_{N_1 3} & U_{N_1 4} & U_{N_1 5} & U_{N_1 6} \\ U_{N_2 1} & U_{N_2 2} & U_{N_2 3} & U_{N_2 4} & U_{N_2 5} & U_{N_2 6} \\ U_{N_3 1} & U_{N_3 2} & U_{N_3 3} & U_{N_3 4} & U_{N_3 5} & U_{N_3 6} \end{pmatrix} \begin{pmatrix} \nu_1 \\ \nu_2 \\ \nu_3 \\ \nu_4 \\ \nu_5 \\ \nu_6 \end{pmatrix}, \quad (2.21)$$

where  $N_i$  and  $\nu_{i+3}$  ( $i \in [1, 2, 3]$ ) are the sterile flavor states and the additional RH mass states, respectively. In the  $\nu$ MSM, the two heavy RH neutrinos generate the active neutrino masses through the type I seesaw mechanism [30–34], where they are assumed to be SM scalars and couple to the Higgs field as such.

### 2.2.3 Observational Avenues for Right-Handed Neutrinos

If the RH neutrinos have masses at the eV scale, they can be observed through distortion effects in measurements of neutrino oscillation experiments. Several analyses looking for these so-called light sterile neutrinos exist in IceCube, where [35] is using atmospheric neutrinos in the higher energy range of 500 GeV to 10 000 GeV and [19] is using the lower energy region of 6 GeV to 156 GeV. The latter work includes a detailed description of the expected oscillation effects and the various anomalies observed in oscillation experiments that could be explained by the existence of a light sterile neutrino, which is not covered in this work.

Here, the focus will be on heavy RH neutrinos, interchangeably also called heavy sterile neutrinos, or HNLs. A defining property is that they are too massive to be produced in oscillations and to be observed as distortions thereof. Several ways to observe HNLs are possible through direct production and decay experiments, which will be discussed in the following. Most of the existing searches assume the minimal model, where only one coupling between the new mass states and the SM neutrinos is non-zero and the coupling is just through mass mixing in a type I seesaw scenario, but more complex scenarios are of course also possible and might produce various additional signatures, or stronger signals.

In general, the constraints discussed in the following are based on models, where only the coupling between the HNL and one SM flavor is non-zero. While this is the straight forward approach to test the mixing parameters individually, this might make the constraints stronger than they would be in a more complex scenario, where the HNLs couple to more than one SM flavor as was shown in [36] for collider bounds.

[28]: Asaka et al. (2005), “The nuMSM, dark matter and neutrino masses”

[29]: Asaka et al. (2005), “The  $\nu$ MSM, dark matter and baryon asymmetry of the universe”

elaborate on Leptogenesis in  $\nu$ MSM and sterile neutrino DM, or link some papers? (ORANGE)

[30]: Minkowski (1977), “ $\mu \rightarrow e \gamma$  at a rate of one out of  $10^9$  muon decays?”

[31]: Yanagida (1980), “Horizontal Symmetry and Masses of Neutrinos”  
[32]: Glashow (1980), “The Future of Elementary Particle Physics”  
[33]: Gell-Mann et al. (1979), “Complex Spinors and Unified Theories”  
[34]: Mohapatra et al. (1980), “Neutrino Mass and Spontaneous Parity Nonconservation”

I think here I'd want the extended leptonic EW lagrangian, so I can explain the mass mixing and the interactions it opens up (RED)

[35]: Aartsen et al. (2020), “eV-Scale Sterile Neutrino Search Using Eight Years of Atmospheric Muon Neutrino Data from the IceCube Neutrino Observatory”

[19]: Trettin (2023), “Search for eV-scale sterile neutrinos with IceCube DeepCore”

[36]: Tastet et al. (2021), “Reinterpreting the ATLAS bounds on heavy neutral leptons in a realistic neutrino oscillation model”

### Extracted Beamline Searches

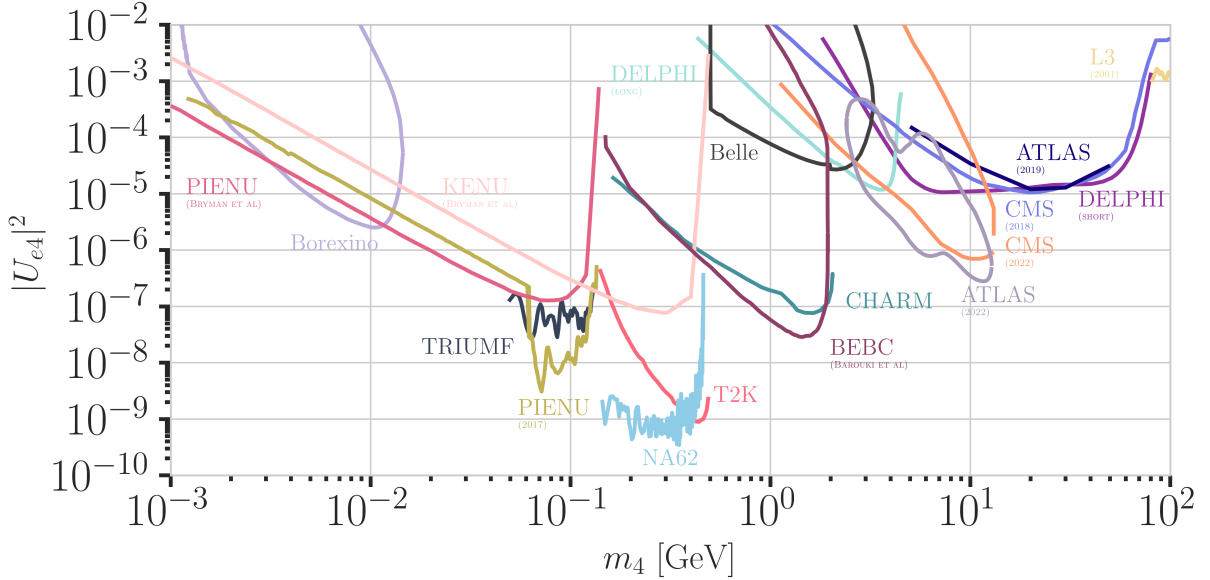


**Figure 2.2:** Current leading  $|U_{e4}^2| - m_4$  limits from PIENU [37, 38], BOREXINO [39], KENU , TRIUMF [40], NA62 [41], T2K [42], DELPHI [43], BEBC [44], Belle , L3 , CHARM [45], ATLAS [46, 47], CMS [48, 49], and NuTeV [50]. Modified from [51].

Protons interacting with a target or a beam dump can produce pions, kaons, and heavy-quark hadrons, whose subsequent decays would also produce HNLs. The energies of the HNLs produced in those interactions are between 1 MeV and 4 GeV and could decay at several distances, depending on their lifetime, which is model dependent. Experiments along the extracted beamline, which are using a spectrometer with particle identification, can search for unique decay signatures at displaced vertices. Example signatures are  $\nu_4 \rightarrow l_\alpha \pi$ ,  $\nu_4 \rightarrow l_\alpha^+ l_\alpha^-$ , or  $\nu_4 \rightarrow \nu \pi^0$  (or other neutral mesons), which cannot be explained by SM neutrinos. Depending on the decay channel, a specific mixing can be probed. The other way of searching for HNLs with these interactions is to look for peaks in the missing mass spectrum, measured around the production vertex at the target, which usually is not possible for beam dumps, as the beam dump region is not calorimetrically instrumented.

HNL search pioneer work was done by experiments at extracted beam lines, with first results from PS191 [52] and CHARM [45], reporting bounds from direct production and decay of HNLs for  $|U_{e4}|^2$ ,  $|U_{\mu 4}|^2$ , and combinations of them, at masses from 10 MeV to 500 MeV at orders of  $10^{-3}$  to  $10^{-6}$ . Since then, there has been and still is a large activity of searches for HNLs at extracted beamlines and the strongest bounds on  $|U_{e4}|^2$  and  $|U_{\mu 4}|^2$  are currently set by PIENU [37, 38, 53], TRIUMF [40], NA62 [41], T2K [42], MicroBooNE [54], and NuTev [50] in the mass range from 1 MeV to 4 GeV, reaching from  $10^{-4}$  at the lower mass to  $10^{-9}$  at 4 at the highest masses. The current strongest bounds are shown in Figure 2.2 and Figure 2.3, which also shows bounds from other experiments, which will be discussed in the following.

Especially noteworthy are the results of analyses probing the mixing with the third lepton generation,  $|U_{\tau 4}|^2$ , from NOMAD [55] and reinterpretations of the CHARM results and the BEBC results in the context of the mixing  $|U_{\tau 4}|^2$ , where the latter is place the most stringent limits from  $10^{-3}$  to  $10^{-6}$

mention KENU, Belle, L3 in the text and add references (RED)

- [52]: Bernardi et al. (1986), "Search for Neutrino Decay"
- [45]: Bergsma et al. (1983), "A Search for Decays of Heavy Neutrinos"
- [37]: Bryman et al. (2019), "Constraints on Sterile Neutrinos in the MeV to GeV Mass Range"
- [38]: Aguilar-Arevalo et al. (2018), "Improved search for heavy neutrinos in the decay  $\pi \rightarrow e\nu$ "
- [53]: Ito et al. (2021), "Search for heavy neutrinos in  $\pi^+ \rightarrow \mu^+ \nu$  decay and status of lepton universality test in the PIENU experiment"
- [40]: Britton et al. (1992), "Improved search for massive neutrinos in  $\pi^+ \rightarrow e + \nu$  decay"
- [41]: Parkinson et al. (2022), "Search for heavy neutral lepton production at the NA62 experiment"
- [42]: Abe et al. (2019), "Search for heavy neutrinos with the T2K near detector ND280"
- [54]: Abratenko et al. (2024), "Search for Heavy Neutral Leptons in Electron-Positron and Neutral-Pion Final States with the MicroBooNE Detector"
- [50]: Vaitaitis et al. (1999), "Search for neutral heavy leptons in a high-energy neutrino beam"
- [55]: Astier et al. (2001), "Search for heavy neutrinos mixing with tau neutrinos"

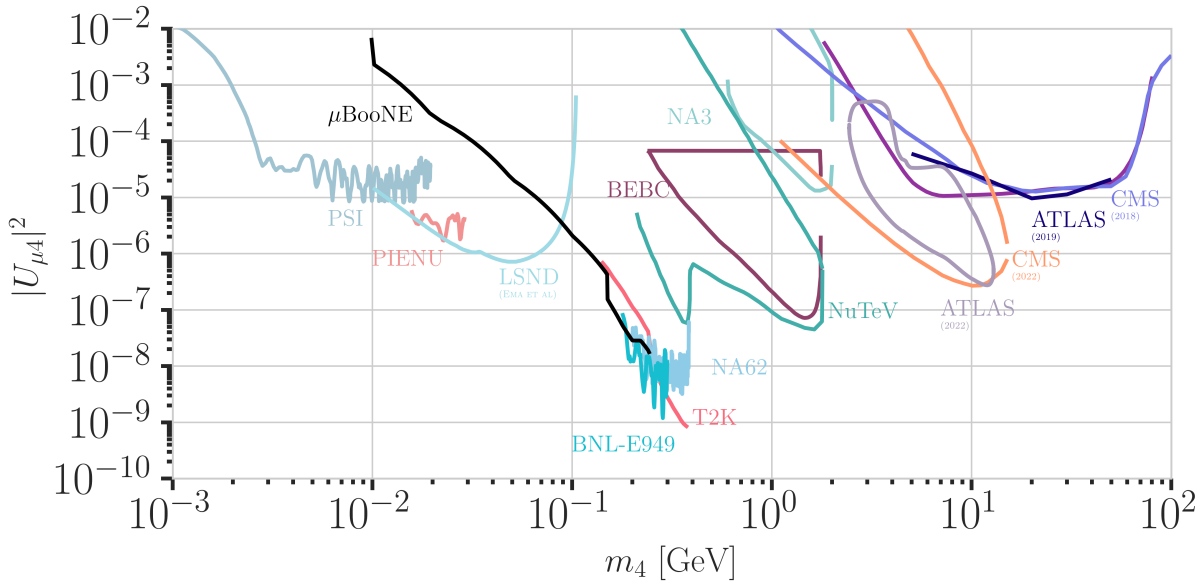


**Figure 2.3:** Current leading  $|U_{\mu 4}^2| - m_4$  limits from PSI ,  $\mu$ BooNE [54], PIENU [37], LSND , BNL-E949 , NA62 [41], T2K [42], BEBC [58], ATLAS [46, 47], CMS [48, 49], NuTeV [50], and NA3 . Modified from [51]. Modified from [51].

[44]: Barouki et al. (2022), “Blast from the past II: Constraints on heavy neutral leptons from the BEBC WA66 beam dump experiment”

[56]: Orloff et al. (2002), “Limits on the mixing of tau neutrino to heavy neutrinos”

[57]: Boiarska et al. (2021), “Blast from the past: constraints from the CHARM experiment on Heavy Neutral Leptons with tau mixing”

mention PSI, LSND, BNL, NA3 in the text and add references (RED)

[46]: Aad et al. (2019), “Search for heavy neutral leptons in decays of W bosons produced in 13 TeV  $p\bar{p}$  collisions using prompt and displaced signatures with the ATLAS detector”

[47]: Aad et al. (2023), “Search for Heavy Neutral Leptons in Decays of W Bosons Using a Dilepton Displaced Vertex in  $\sqrt{s} = 13$ TeV  $p\bar{p}$  Collisions with the ATLAS Detector”

[48]: Sirunyan et al. (2018), “Search for heavy neutral leptons in events with three charged leptons in proton-proton collisions at  $\sqrt{s} = 13$  TeV”

[49]: Tumasyan et al. (2022), “Search for long-lived heavy neutral leptons with displaced vertices in proton-proton collisions at  $\sqrt{s} = 13$  TeV”

[59]: Shuve et al. (2016), “Revision of the LHCb Limit on Majorana Neutrinos”

[60]: Aaij et al. (2021), “Search for heavy neutral leptons in  $W^+ \rightarrow \mu^+ \mu^\pm$ jet decays”

in the 0.1 GeV to 2 GeV range [44, 56, 57]. In Figure 2.4 the current strongest bounds on  $|U_{\tau 4}|^2$  are shown.

### Collider Searches

So far, collider searches have been conducted at the *large electron positron collider (LEP)* and at the *large hadron collider (LHC)* in proton-proton mode. Strongest results are from the *ATLAS* and *CMS* experiments, which are nearly hermetic, general purpose detectors around the interaction point, and from the *DELPHI* and the *LHCb* experiments, which are forward detectors that can be used to search for new particles in decays of heavy particles produced. In the minimal model, HNLs in the GeV mass range can be produced through mass mixing in decays of heavy mesons, tau leptons, Z/W bosons, H bosons, or top quarks originating from the collisions. Depending on the dirac or majorana nature of the HNL, they can decay to lepton number conserving or lepton number violating channels.

Using prompt and displaced decays of the HNL, both ATLAS and CMS have set constraints on  $|U_{e4}|^2$  and  $|U_{\mu 4}|^2$  at the level of  $10^{-4}$  to  $10^{-6}$  in the mass range between 1 GeV to 100 GeV [46–49]. The LHCb experiment has HNL search results at HNL masses below and above the W boson mass, where the low mass searches are using the decay channel  $B^- \rightarrow \pi^+ \mu^- \mu^-$ , setting limits at the  $10^{-3}$  level for  $|U_{\mu 4}|^2$  in the mass range of 0.5 GeV to 3.5 GeV [59]. At high masses, the  $W^+ \rightarrow \mu^- \mu^\pm$ jet channel is used to set limits at the order of  $10^{-3}$  to  $10^{-2}$  for  $|U_{\mu 4}|^2$  in the mass range of 5 GeV to 50 GeV in the LNC channel and at the order of  $10^{-4}$  to  $10^{-3}$  in the LNV channel [60].

### Nuclear Decays Measurements

A novel approach of searching for irregularities in energy-momentum conservation measurements in nuclear reactions might be a viable way of

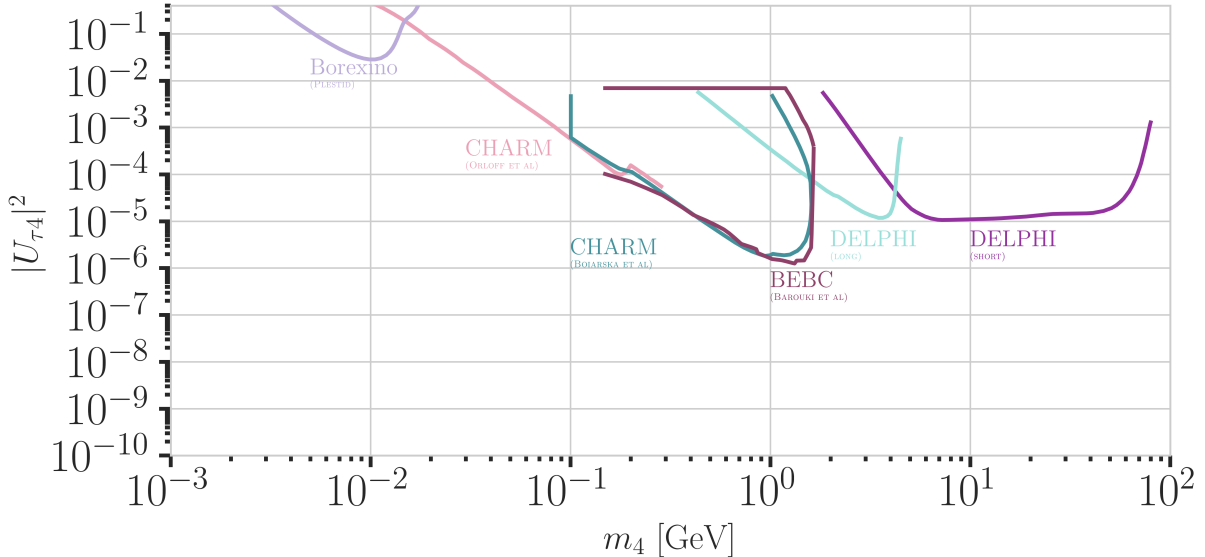


**Figure 2.4:** Current leading  $|U_{\tau 4}^2| - m_4$  limits from BOREXINO [61], CHARM [56, 57], DELPHI [43], and BEBC [44]. Modified from [51].

searching for HNLs, as they could be interpreted as constraints on  $|U_{e4}|^2$  and  $m_4$ .

Kinks in **beta decay** spectra would show up at  $Q - m_4 c^2$ , where the HNL mass,  $m_4$ , can be measured between the lower energy detection threshold and the energy released in the decay, which is called  $Q$  value. Analyses using the tritium decay, with  $Q = 18.6$  keV, are planned in *KATRIN* [62] and *TRISTAN* [63] in the 1 keV to 18 keV range. Their projected statistical limits are around  $10^{-7}$  for  $|U_{e4}|^2$ , but will require further detector upgrades [63]. A first result from KATRIN measurements during commissioning sets limits at the order of  $10^{-2}$  to  $10^{-3}$  in the mass range of 0.1 keV to 1.6 keV [64]. *DUNE* is planning to measure the ionization charge of atmospheric argon decays, with  $Q = 565$  keV, to probe  $|U_{e4}|^2$  at in the 20 keV to 450 keV mass range. The projected sensitivity is at the  $10^{-5}$  level, and might improve to  $10^{-7}$  with additional detector improvements [65].

mention the Z boson decay results from DELPHI (because they are strong in Utau4, too (RED))

[62]: Osipowicz et al. (2001), "KATRIN: A Next generation tritium beta decay experiment with sub-eV sensitivity for the electron neutrino mass. Letter of intent"

[63]: Mertens et al. (2019), "A novel detector system for KATRIN to search for keV-scale sterile neutrinos"

[64]: Aker et al. (2023), "Search for keV-scale sterile neutrinos with the first KATRIN data"

[65]: Abi et al. (2020), "Deep Underground Neutrino Experiment (DUNE), Far Detector Technical Design Report, Volume II: DUNE Physics"

To test for the existence of HNLs using **electron capture** measurements, total energy-momentum reconstruction of all non-neutrino final states is needed. Electron capture is a pure two body decay process, where the recoiling atom and the electron neutrino are the only final state particles, but additional energy is carried away by the de-excitation x-ray or auger electron. The energy-momentum conservation can be probed by measuring the atom and the associated de-excitation products. The mixing  $|U_{e4}|^2$  can be probed by looking for a separated non-zero missing mass peak. The *BeEST* experiment has set limits at the  $10^{-4}$  level in the 100 keV to 850 keV mass range, using berillium-7, which has a  $Q$  value of 862 keV. After planned upgrades to the experiment, the sensitivity is expected to improve to the  $10^{-7}$  level [66].

**Reactor searches** up to 12 MeV in mass are possible at short baseline experiments using commercial or research reactors, which are a strong source of electron antineutrinos and could therefore also produce HNLs if  $|U_{e4}|^2$  is non-zero. Visible decay channels at these energies are  $\nu_4 \rightarrow \nu_e e^+ e^-$ ,  $\nu_4 \rightarrow \nu \gamma$ , and  $\nu_4 \rightarrow \nu \gamma \gamma$ , where the first dominates. The first analysis in this field, reports limits at the  $10^{-4}$  level in the 2 MeV to 7 MeV mass range [67].

[66]: Friedrich et al. (2021), "Limits on the Existence of sub-MeV Sterile Neutrinos from the Decay of  ${}^7\text{Be}$  in Superconducting Quantum Sensors"

[67]: Hagner et al. (1995), "Experimental search for the neutrino decay  $v3 + vj + e^+ + e^-$  and limits on neutrino mixing"

## Atmospheric and Solar

Natural sources of neutrinos are provided up to 20 MeV by the sun and up to 100s of GeV by neutrino production in the atmosphere. Both fluxes contain all flavors of neutrinos, due to mixing and oscillations, and can therefore be used to directly probe the mixings with  $\nu_e$ ,  $\nu_\mu$ , and  $\nu_\tau$ . Depending on the HNL mass and the strength of the mixing, which both govern the decay length, different signatures can be used to experimentally access large regions of the HNL parameter space. The strength of the mixing defines the total rate of HNL events, which is additionally affected by whether solely the minimal mass mixing is assumed, or also more complicated mixing scenarios, like the dipole portal, are considered.

So far, only very few analyses exist, which are performed by the experimental collaborations themselves. Several external theoretical groups have predicted the expected sensitivities to HNLs, produced from solar or atmospheric neutrinos, based on various coupling scenarios and decay lengths. A selection of the potential analyses will be discussed in the following.

For very long-lived particles, **production inside the sun** can be used as a source to search for HNLs in detectors on earth. This will only allow production through non-zero  $|U_{e4}|^2$ , because the initial solar neutrino flux is only  $\nu_e$ . By searching for HNL decays to a SM neutrino and an electron positron pair  $\nu_4 \rightarrow \nu_e e^+ e^-$  and comparing to the expected inter planetary positron flux, *Borexino* has placed the strongest limits on the mixing  $|U_{e4}|^2$  a the order of  $10^{-5}$  in the few MeV mass range [39].

For HNL decay length scales of the order of the Earth's diameter, HNL **up-scattering outside the detector** is possible, where a neutrino from the solar or the atmospheric neutrino flux scatters in the Earth and transfers some kinetic energy into the mass of the HNL, which can then later decay inside the detector. For HNL masses below 18 MeV produced from solar neutrinos, (external) limits were derived using the *Borexino* data for purely tau coupling through mass mixing [61] and for all flavor coupling through the dipole portal [68]. At similar decay length scales, the HNL could also be produced directly in the atmosphere, but neither this channel, nor the production anywhere in the Earth from atmospheric neutrinos has been investigated yet.

[39]: Bellini et al. (2013), "New limits on heavy sterile neutrino mixing in B8 decay obtained with the *Borexino* detector"

[61]: Plestid (2021), "Luminous solar neutrinos I: Dipole portals"

[68]: Plestid (2021), "Luminous solar neutrinos II: Mass-mixing portals"

[69]: Coloma et al. (2017), "Double-Cascade Events from New Physics in *Icecube*"

[70]: Coloma (2019), "Icecube/Deep-Core tests for novel explanations of the *MiniBooNE* anomaly"

[71]: Atkinson et al. (2022), "Heavy Neutrino Searches through Double-Bang Events at Super-Kamiokande, DUNE, and Hyper-Kamiokande"

[72]: Coloma et al. (2021), "GeV-scale neutrinos: interactions with mesons and DUNE sensitivity"

If the HNL decay lengths are sufficiently short, **production and decay in the detector** can happen and the observation of two vertices could be used to constrain the mixing parameters. In principle, this could be possible with any neutrino flavor produced in the sun or the atmosphere, but so far only theoretical studies have been performed for mass-mixing and dipole-portal couplings for the atmospheric neutrino detectors *IceCube* [69, 70] and *Super-K*, *Hyper-K*, and *Dune* [71, 72]. Due to the high complexity of these experiments, several simplified assumptions were made in the studies, which might not hold in reality, and the results should be taken with caution. For reliable sensitivity estimates and limits the collaborations should perform their own analyses.

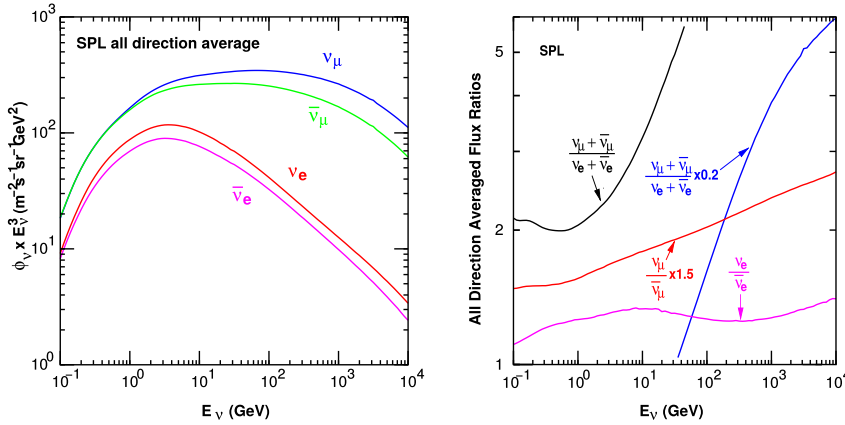


**Figure 2.5:** The atmospheric fluxes of different neutrino flavors as a function of energy (left) and the ratios between muon neutrinos and electron neutrinos as well as the ratios between neutrinos and antineutrinos for both those flavors (right). Results from the calculations performed for the geographic South Pole, taken from [74].

## 2.3 Atmospheric Neutrinos as Source of Heavy Neutral Leptons

This work focuses on the search for HNLs using atmospheric neutrinos as source for the production and decay inside the IceCube detector. The following sections will give a brief overview of the production of neutrinos in the atmosphere and the oscillations they undergo, before discussing the expected signatures of HNLs in the detector, where they are produced from the incoming neutrinos and subsequently decay.

### 2.3.1 Production of Neutrinos in the Atmosphere

The analysis performed in this work is based on the sample of neutrinos observed in IceCube DeepCore at energies below 100 GeV. At these energies, the flux exclusively originates in the Earth's atmosphere. Highly relativistic cosmic rays (protons and heavier nuclei [73]) interact in the upper atmosphere, producing showers of secondary particles. Neutrinos are produced in decays of charged pions and kaons ( $\pi$  and  $K$  mesons) present in those showers, where the dominant contribution comes from the decay chain

$$\begin{aligned} \pi^\pm &\rightarrow \mu^\pm + \nu_\mu (\bar{\nu}_\mu), \\ \mu^\pm &\rightarrow e^\pm + \bar{\nu}_\mu (\nu_\mu) + \nu_e (\bar{\nu}_e), \end{aligned} \quad (2.22)$$

where muon neutrinos  $\nu_\mu$  and muons  $\mu^\pm$  are produced in the first decay and both electron and muon neutrinos  $\nu_{e/\mu}$  are produced in the second decay. Atmospheric muons, which are also produced in these decays, are the main background component for IceCube DeepCore analyses.

The different atmospheric flux components are shown in Figure 2.5 (left), for a much broader energy range than relevant for this work. Both neutrinos and antineutrino fluxes are shown for electron and muon neutrinos and all fluxes are the directionally averaged expectation calculated at the South Pole. Muon neutrinos are dominating the flux and from Equation 2.22 the naive assumption would be that the ratio between muon and electron neutrinos is  $(\nu_\mu + \bar{\nu}_\mu)/(\nu_e + \bar{\nu}_e) = 2$ . This is roughly true at energies below 1 GeV, where all muons decay in flight, but at larger energies muons can reach the detector before decaying, which increases the ratio to approximately 10:1 at around 100 GeV. Additionally, kaon decays start to contribute which also increases the number of muons and muon neutrinos. The increasing ratio can be seen

[73]: Tanabashi et al. (2018), "Review of Particle Physics"

in Figure 2.5 (right), which also shows the ratio between neutrinos and antineutrinos for both flavors.

[75]: Fedynitch et al. (2015), “Calculation of conventional and prompt lepton fluxes at very high energy”

Say something about atmospheric neutrino flux uncertainties, based on recent JP/Anatoli papers. (YELLOW)

Charged mesons or tau particles can also be produced in cosmic ray interactions. Their decays lead to the production of tau neutrinos. At the energies relevant for this work however, the resulting tau neutrino flux is negligible as compared to the muon neutrino flux [75] and is not considered in the analysis. This is because both charged mesons and tau particles are much heavier than pions and kaons and therefore their production is suppressed at high energies.

### 2.3.2 Neutrino Oscillations

Describing neutrinos in their mass state as introduced in Section ?? is crucial to understand their propagation through space and time and to explain neutrino oscillations. Oscillations mean that a neutrino changes from its initial flavor, that it was produced with, to another flavor and back after traveling a certain distance.

The neutrino propagation in vacuum can be expressed by applying a plane wave approach, where the mass eigenstates evolve as

$$|\nu_k(t)\rangle = e^{-iE_k t/\hbar} |\nu_k\rangle . \quad (2.23)$$

The energy of the mass eigenstate  $|\nu_k\rangle$  is  $E_k = \sqrt{\vec{p}^2 c^2 + m_k^2 c^4}$ , with momentum  $\vec{p}$  and mass  $m_k$ ,  $\hbar$  is the reduced Planck constant, and  $c$  is the speed of light in vacuum. A neutrino is produced as a flavor eigenstate  $|\nu_\alpha\rangle$  in a CC weak interaction, but its propagation happens as the individual mass states it is composed of. The probability of finding the neutrino with initial flavor  $|\nu_\alpha\rangle$  in the flavor state  $|\nu_\beta\rangle$  after the time  $t$  is calculated as

$$P_{\nu_\alpha \rightarrow \nu_\beta}(t) = |\langle \nu_\beta | \nu_\alpha(t) | \nu_\beta \rangle|^2 , \quad (2.24)$$

[76]: Dirac (1927), “The Quantum Theory of the Emission and Absorption of Radiation”

by applying Fermi’s Golden Rule [76], which defines the transition rate from one eigenstate to another by the strength of the coupling between them. This coupling strength is the square of the matrix element and using the fact that the mixing matrix is unitary ( $U^{-1} = U^\dagger$ ) to describe the mass eigenstates as flavor eigenstates, we find the time evolution of the flavor state  $|\nu_\alpha(t)\rangle$ , which can be inserted into Equation 2.24 to find the probability as

$$P_{\nu_\alpha \rightarrow \nu_\beta}(t) = \sum_{j,k} U_{\beta j}^* U_{\alpha j} U_{\beta k} U_{\alpha k}^* e^{-i(E_k - E_j)t/\hbar} . \quad (2.25)$$

The indices  $j$  and  $k$  run over the mass eigenstates.

We can approximate the energy as

$$E_k \approx E + \frac{c^4 m_k^2}{2E} \longrightarrow E_k - E_j \approx \frac{c^4 \Delta m_{kj}^2}{2E} , \quad (2.26)$$

for small neutrino masses compared to their kinetic energy. Here,  $\Delta m_{kj}^2 = m_k^2 - m_j^2$  is the mass-squared splitting between states  $k$  and  $j$ . Replacing the time in Equation 2.25 by the distance traveled by relativistic neutrinos

$t \approx L/c$  we get

$$\begin{aligned} P_{\nu_\alpha \rightarrow \nu_\beta}(t) &= \delta_{\alpha\beta} - 4 \sum_{j>k} \text{Re}(U_{\beta j}^* U_{\alpha j} U_{\beta k} U_{\alpha k}^*) \sin^2 \left( \frac{c^3 \Delta m_{kj}^2}{4E\hbar} L \right) \\ &\quad + 2 \sum_{j>k} \text{Im}(U_{\beta j}^* U_{\alpha j} U_{\beta k} U_{\alpha k}^*) \sin^2 \left( \frac{c^3 \Delta m_{kj}^2}{4E\hbar} L \right), \end{aligned} \quad (2.27)$$

which is called the survival probability if  $\alpha = \beta$ , and the transition probability if  $\alpha \neq \beta$ . Once again, this probability is only non-zero if there are neutrino mass eigenstates with masses greater than zero. Additionally, there must be a mass-squared difference  $\Delta m^2$  and non-zero mixing between the states. Since we assumed propagation in vacuum in Equation 2.23, the transition and survival probabilities correspond to vacuum mixing.

[73]: Tanabashi et al. (2018), "Review of Particle Physics"

The mixing matrix can be parameterized as [73]

$$U = \begin{pmatrix} 1 & 0 & 0 \\ 0 & c_{23} & s_{23} \\ 0 & -s_{23} & c_{23} \end{pmatrix} \begin{pmatrix} c_{13} & 0 & s_{13} e^{-i\delta_{CP}} \\ 0 & 1 & 0 \\ -s_{13} e^{i\delta_{CP}} & 0 & c_{13} \end{pmatrix} \begin{pmatrix} c_{12} & s_{12} & 0 \\ -s_{12} & c_{12} & 0 \\ 0 & 0 & 1 \end{pmatrix}, \quad (2.28)$$

where  $c_{ij} = \cos \theta_{ij}$  and  $s_{ij} = \sin \theta_{ij}$  are cosine and sine of the mixing angle  $\theta_{ij}$ , that defines the strength of the mixing between the mass eigenstates  $i$  and  $j$ , and  $\delta_{CP}$  is the neutrino CP-violating phase. Experiments are sensitive to different mixing parameters, depending on the observed energy range, neutrino flavor, and the distance between the source and the detector  $L$ , commonly referred to as *baseline*. To be able to resolve oscillations the argument

$$\frac{\Delta m^2 L}{4E} \quad (2.29)$$

should be at the order of 1. This divides experiments into ones that are sensitive to very slow oscillations from  $\Delta m_{21}^2 \approx \mathcal{O}(10^{-5} \text{eV}^2)$  and ones that are sensitive to faster oscillations from  $\Delta m_{31}^2 \approx \mathcal{O}(10^{-3} \text{eV}^2)$ . Relevant for this work are the parameters that can be measured at the earth's surface using atmospheric neutrinos, which are  $\Delta m_{31}^2$ ,  $\theta_{23}$ , and  $\theta_{13}$ , because the flux is primarily composed of muon neutrinos and antineutrinos. Applying the parameterization from Equation 2.28 to Equation 2.27 and using the fact that  $\theta_{13}$  is small and  $\theta_{12}$  is close to  $\pi/4$ , the survival probability of muon neutrinos can be approximated as

$$\begin{aligned} P_{\nu_\mu \rightarrow \nu_\mu} &\simeq 1 - 4|U_{\mu 3}|^2(1 - |U_{\mu 3}|^2) \sin^2 \left( \frac{\Delta m_{31}^2 L}{4E} \right) \\ &\simeq 1 - \sin^2(2\theta_{23}) \sin^2 \left( \frac{\Delta m_{31}^2 L}{4E} \right), \end{aligned} \quad (2.30)$$

while the tau neutrino appearance probability is

$$\begin{aligned} P_{\nu_\mu \rightarrow \nu_\tau} &\simeq 4|U_{\mu 3}|^2|U_{\tau 3}|^2 \sin^2 \left( \frac{\Delta m_{31}^2 L}{4E} \right) \\ &\simeq \sin^2(2\theta_{23}) \sin^2 \left( \frac{\Delta m_{31}^2 L}{4E} \right). \end{aligned} \quad (2.31)$$

The latest global fit [77] of all the parameters is shown in Table 2.2.

Parameter	Global Fit
$\theta_{12}$ [°]	$33.41^{+0.75}_{-0.72}$
$\theta_{13}$ [°]	$8.54^{+0.11}_{-0.10}$
$\theta_{23}$ [°]	$49.1^{+1.0}_{-1.3}$
$\Delta m_{21}^2$ [ $10^{-5} \text{eV}^2$ ]	$7.41^{+0.21}_{-0.20}$
$\Delta m_{31}^2$ [ $10^{-3} \text{eV}^2$ ]	$2.511^{+0.028}_{-0.027}$
$\delta_{CP}$ [°]	$197^{+42}_{-25}$

Table 2.2: Results from the latest global fit of neutrino mixing parameters from [77].

[77]: Esteban et al. (2020), "The fate of hints: updated global analysis of three-flavor neutrino oscillations"

say something about matter effect? (ORANGE)

say something about mass ordering? (ORANGE)

### 2.3.3 Neutrino Interactions with Nuclei

The neutrino detection principle of IceCube DeepCore is explained in Chapter ?? and relies on the weak interaction processes between neutrinos and the nuclei of the Antarctic glacial ice. At neutrino energies above 5 GeV, the cross-sections are dominated by *deep inelastic scattering (DIS)*, where the neutrino is energetic enough to resolve the underlying structure of the nucleons and interact with one of the composing quarks individually. As a result the nucleon breaks and a shower of hadronic secondary particles is produced. Depending on the type of interaction, the neutrino either remains in the final state for NC interactions or is converted into its charged lepton counterpart for CC interactions. The CC DIS interactions have the form

$$\begin{aligned} \nu_l + N &\rightarrow l^- + X , \\ \bar{\nu}_l + N &\rightarrow l^+ + X , \end{aligned} \quad (2.32)$$

where  $\nu_l/\bar{\nu}_l$  and  $l^-/l^+$  are the neutrino/antineutrino and its corresponding lepton/antilepton, and  $l$  can be either an electron, muon, or tau.  $N$  is the nucleon and  $X$  stands for any set of final state hadrons. The NC DIS interactions are

$$\begin{aligned} \nu_l + N &\rightarrow \nu_l + X \text{ and} \\ \bar{\nu}_l + N &\rightarrow \bar{\nu}_l + X . \end{aligned} \quad (2.33)$$

Figure 2.6 shows the Feynman diagrams for both processes DIS interactions

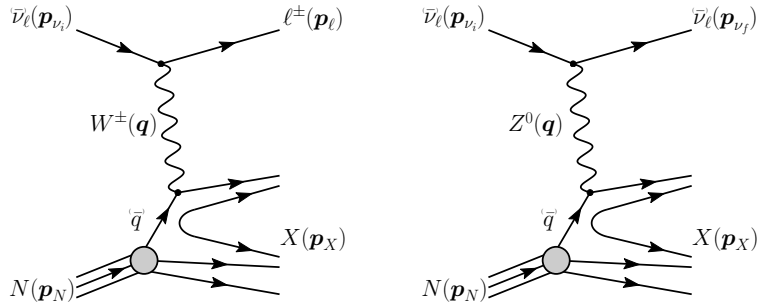


**Figure 2.6:** Feynman diagrams for deep inelastic scattering of a neutrino with a nucleon via charged-current (left) and neutral current (right) interactions.  $p_{\nu_i}, p_N$  and  $p_{\nu_f}$ ,  $p_l$ ,  $p_N$  are the input and output four-momenta, while  $q$  is the momentum transfer. Taken from [78].

have a roughly linear energy dependent cross-section above  $\sim 20$  GeV and are well measured and easy to theoretically calculate. They are the primary interaction channel for neutrinos detected with IceCube.

At energies below 5 GeV, *quasi-elastic scattering (QE)* and *resonant scattering (RES)* become important. At these energies the neutrinos interact with the approximately point-like nucleons, without breaking them up in the process. RES describes the process of a neutrino scattering off a nucleon producing an excited state of the nucleon in addition to a charged lepton. It is the dominant process at 1.5 GeV to 5 GeV for neutrinos and 1.5 GeV to 8 GeV for antineutrinos. Below 1.5 GeV QE is the main process, where protons are converted to neutrons in antineutrino interactions and vice-versa for neutrino interactions. Additionally, a charged lepton corresponding to the neutrino/antineutrino flavor is produced. The cross-sections of QE and RES scattering processes are not linear in energy and the transition region from QE/RES to DIS is poorly understood. The total cross-sections and their composition is shown in Figure 2.7. It can be seen that the interaction cross-sections are very small at the order of  $10^{-38}$  cm $^2$ . This is the reason why very

large volume detectors are required to measure atmospheric neutrinos with sufficient statistics to perform precision measurements of their properties. The interaction length of a neutrino with  $E_\nu = 10 \text{ GeV}$  is of  $\mathcal{O}(10 \times 10^{10} \text{ km})$ , for example.

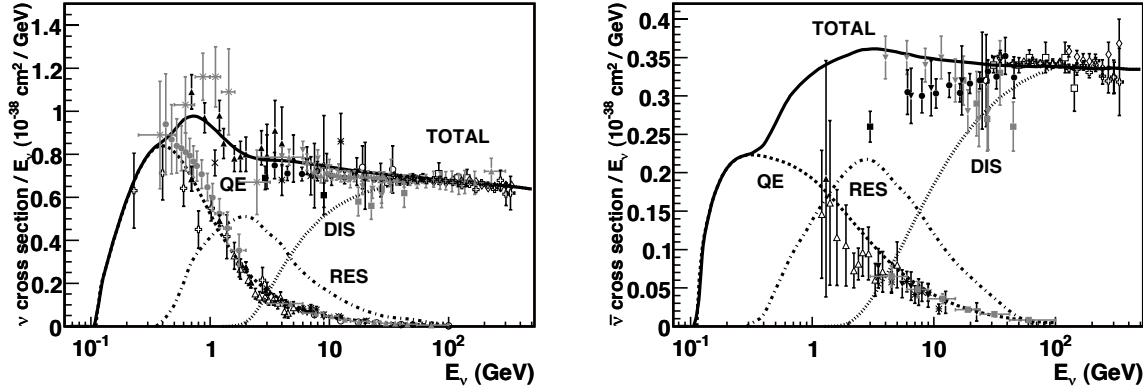


**Figure 2.7:** Total neutrino (left) and antineutrino (right) per nucleon cross-section divided by neutrino energy plotted against energy. The three main scattering processes quasi-elastic scattering (QE), resonant scattering (RES), and deep-inelastic scattering (DIS) are shown. Taken from [79].

### 2.3.4 Heavy Neutral Lepton Production and Decay

For the search conducted in this work, both production and decay are assumed to happen inside the detector, therefore probing decay lengths ranges at the scale of the detector size, which is below 1000 m. Since the mixing with the first two generations of leptons is already strongly constrained as was discussed in Section 2.3, only the mixing with the tau neutrino will be considered in the following. Due to the effect of oscillations, described in Section 2.3.2, the initial atmospheric muon neutrino flux provides a sizable tau neutrino flux at the detector.

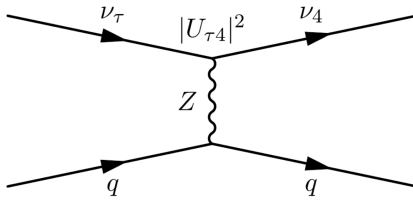


**Figure 2.8:** Feynman diagram of the HNL production. The heavy mass state is produced in the up-scattering of a tau neutrino.

For a non-zero  $|U_{\tau 4}|^2$ , the HNL can be produced through **up-scattering in the ice**. An incoming tau neutrinos scatters on an ice nucleus and transfers some of its kinetic energy to the heavy neutrino. The Feynman diagram of this process is shown in Figure 2.8. The custom NC cross-sections calculated for this purpose are explained in more detail in Section ??, but are similar to the SM tau neutrino NC cross-sections, with a reduction scaling with the mixing  $|U_{\tau 4}|^2$  and energy dependent reductions, due to kinematic constraints because of the heavy neutrino mass. The scattering process produces a hadronic cascade, which will produce light in the detector.

After a certain distance, the HNL will **decay in the ice**, where the possible decay channels considered in this work are shown in Figure 2.9 and the underlying, explicit calculations are discussed in Section ???. The decay can be a CC or NC and both purely leptonic and leptonic+mesonic modes

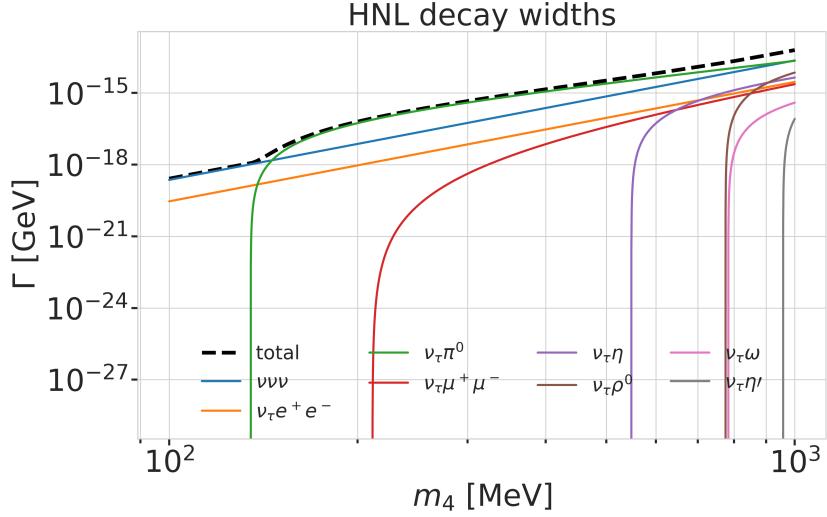
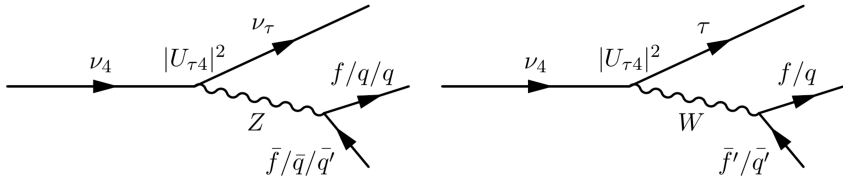


**Figure 2.9:** Decay widths of the HNL within the mass range considered, calculated based on the results from [72]. Given the existing constraints on  $|U_{e4}|^2$  and  $|U_{\mu 4}|^2$ , we consider that the corresponding decay modes are negligible.

**Figure 2.10:** Feynman diagram of the HNL decay. The heavy mass state can decay through neutral current interaction (left) into a tau neutrino and a charged lepton or quark pair, or through charged current interaction (right) into a tau lepton and a charged lepton or quark.



are possible. The Feynman diagrams of the decays can be seen in Section ???. Only the mass range relevant for this work is presented and mixing with  $\nu_{e/\mu}$  is assumed to be negligible. Depending on the decay channel, an electromagnetic or a hadronic cascade is produced, while some energy is carried away by the invisible neutrino. The decay length of the HNL is defined by its proper lifetime<sup>1</sup>, which is given by

$$\tau_{\text{proper}} = \frac{\hbar}{\Gamma_{\text{total}}(m_4) \cdot |U_{\tau 4}|^2}, \quad (2.34)$$

where  $\hbar$  is the reduced Planck constant,  $\Gamma_{\text{total}}(m_4)$  is the total decay width of the HNL for the given mass, and  $|U_{\tau 4}|^2$  is the mixing with the tau neutrino. The total decay width is the sum of the partial decay widths for all possible decay channels. The mean lab frame decay length is then given by

$$L_{\text{decay}} = \gamma v \tau_{\text{proper}}, \quad (2.35)$$

where  $\gamma$  is the Lorentz factor of the HNL, defined by the kinetic energy. This will be further discussed on Section ???. Figure 2.11 shows the mean decay lengths for an example mass of  $m_4 = 0.6$  GeV and several mixing values.

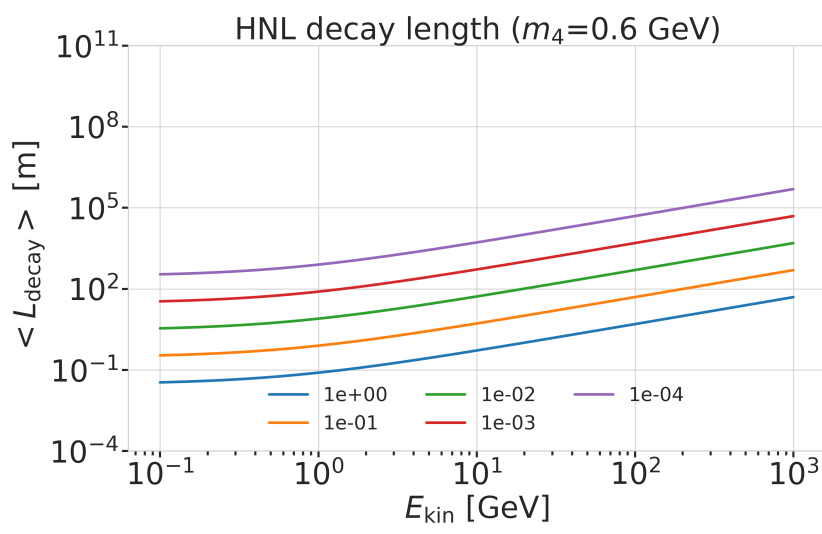


**Figure 2.11:** Theoretical mean decay length of the HNL for a mass of 0.6 GeV and different mixing values.



# Search for Tau Neutrino Induced Heavy Neutral Lepton Events

# 3

This chapter describes the search for HNL events using 10 years of IceCube DeepCore data. The expected number of HNL events in the data sample depends on the mass of the additional heavy state,  $m_4$ , and the mixing element  $|U_{\alpha 4}^2|$ , with  $\alpha = e, \mu, \tau$ , between the SM flavors and the new mass state. As discussed in Section 2.3, this work focuses on the mixing to the tau sector,  $|U_{\tau 4}^2|$ , which has the weakest constraints to date. Since the mass itself influences the production and decay kinematics of the event and the accessible decay modes, individual mass samples were produced as described in Section ???. The mass influences the decay length and energy distributions, while the mixing both changes the overall expected rate of the HNL events and the shape in energy and length. We perform three independent searches for each mass sample, where the mixing is measured in each of the fits.

## 3.1 Final Level Sample

The final level simulation sample of this analysis consists of the neutrino and muon MC introduced in Section ?? and one of the three HNL samples explained in Section ??, while the data are the events measured in 10 years of IceCube DeepCore data taking. All simulation and the data are processed through the full event selection chain described in Section ?? and Section ?? leading to the final level sample. As described in Section ??, event triggers consisting purely of random coincidences induced by noise in the DOMs have been reduced to a negligible rate, and will not be discussed further.

To get the neutrino expectation, the MC events are weighted according to their generation weight introduced in Section ??, multiplied by the total lifetime, and the expected neutrino flux. For the correct expectation at the detector, the events have to be weighted by the oscillation probability, depending on their energy and their distance traveled from the atmosphere to the detector. The oscillation probabilities are calculated using a PYTHON implementation of the calculations from [80], which use the matter profile of the Earth following the *Preliminary Reference Earth Model (PREM)* [81] as input. Apart from the energy and the distance, the two relevant parameters defining the oscillation probabilities are the atmospheric neutrino oscillation parameters  $\theta_{23}$  and  $\Delta m_{31}^2$ . Since the HNL events originate from the tau neutrinos that were produced as muon neutrinos in the atmosphere and then oscillated into  $\nu_\tau$ , this weighting is also applied in addition to the specific weighting scheme for the HNL events described in Section ??, which itself is defined by the mixing  $|U_{\tau 4}^2|$  and the mass  $m_4$ .

3.1	Final Level Sample	21
3.2	Statistical Analysis	24
3.3	Analysis Checks	27
3.4	Results	29
3.5	Outlook	31

[80]: Barger et al. (1980), “Matter effects on three-neutrino oscillations”

[81]: Dziewonski et al. (1981), “Preliminary reference Earth model”

### 3.1.1 Expected Rates/Events

The rates and the expected number of events for the SM background are shown in Table 3.1 with around 175000 total events expected in the 10 years. Only data marked as good is used for the analysis, where *good* refers to

measurement time with the correct physics run configuration and without other known issues. The resulting good detector livetime in this data taking period was 9.28 years. The rates are calculated by summing the weights of all events in the final level sample, while the uncertainties are calculated by taking the square root of the sum of the weights squared. The expected number of events is calculated by multiplying the rate with the livetime. The individual fractions show that this sample is neutrino dominated where the majority of events are  $\nu_\mu$ -CC events.

**Table 3.1:** Final level rates and event expectation of the SM background particle types.

Type	Rate [mHz]	Events (9.28 years)	Fraction [%]
$\nu_\mu^{\text{CC}}$	0.3531	$103321 \pm 113$	58.9
$\nu_e^{\text{CC}}$	0.1418	$41490 \pm 69$	23.7
$\nu^{\text{NC}}$	0.0666	$19491 \pm 47$	11.1
$\nu_\tau^{\text{CC}}$	0.0345	$10094 \pm 22$	5.8
$\mu_{\text{atm}}$	0.0032	$936 \pm 15$	0.5
total	0.5992	$175332 \pm 143$	100.0

Table 3.2 shows the rates and expected number of events for the HNL signal simulation. The expectation depends on the mass and the mixing and shown here are two example mixings for all the three masses that are being tested in this work. A mixing of 0.0 would result in no HNL events at all. It can already be seen that for the smaller mixing of  $|U_{\tau 4}|^2 = 10^{-3}$  the expected number of events is very low, while at the larger mixing of  $|U_{\tau 4}|^2 = 10^{-1}$  the number is comparable to the amount of atmospheric muons in the background sample.

**Table 3.2:** Final level rates and event expectations of the HNL signal for all three masses and two example mixing values.

HNL mass	Rate [ $\mu\text{Hz}$ ]	Events (in 9.28 years)
$ U_{\tau 4} ^2 = 10^{-1}$		
0.3 GeV	3.3	$975 \pm 2$
0.6 GeV	3.1	$895 \pm 2$
1.0 GeV	2.5	$731 \pm 2$
$ U_{\tau 4} ^2 = 10^{-3}$		
0.3 GeV	0.006	$1.67 \pm 0.01$
0.6 GeV	0.022	$6.44 \pm 0.01$
1.0 GeV	0.025	$7.27 \pm 0.01$

### 3.1.2 Analysis Binning

[82]: Yu et al. (2023), “Recent neutrino oscillation result with the Ice-Cube experiment”

Add fractions of the different particle types in the bins for benchmark mass/mixing (another table??). Three dimensional binning used in the analysis. All variables are from the DNN reconstruction (ORANGE section ??).

An identical binning to the analysis performed in [82] is used. In total, there are three bins in PID (cascade like, mixed, and track like), 12 bins in reconstructed energy, and 8 bins in cosine of the reconstructed zenith angle as specified in Table 3.3. Extending the binning towards lower energies or

Variable	N <sub>bins</sub>	Edges	Spacing
$P_\nu$	3	[0.00, 0.25, 0.55, 1.00]	linear
$E$	12	[5.00, 100.00]	logarithmic
$\cos(\theta)$	8	[-1.00, 0.04]	linear

increasing the number of bins in energy or cosine of the zenith angle did not improve the HNL sensitivities significantly, because the dominant signal region is already covered with a sufficiently fine binning to observe the shape and magnitude of the HNL events on top of the SM background. This

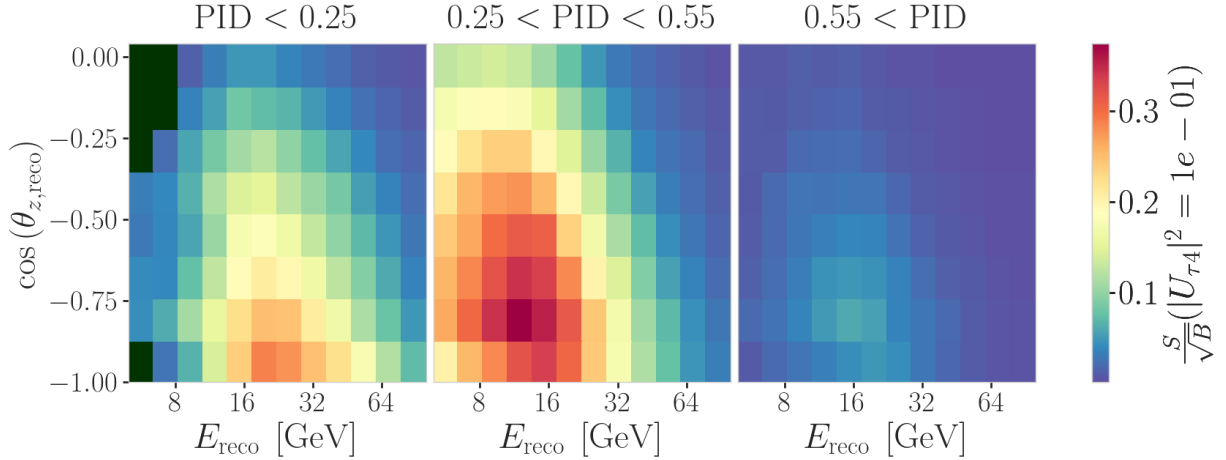


**Figure 3.1:** Signal over square root of background expectation in 9.28 years for the 1.0 GeV mass sample at a mixing of 0.1, while all other parameters are at their nominal values.

can be seen in the middle panel of Figure 3.1, which shows the expected signal events divided by the square root of the expected background events for every bin used in the analysis. The signal expectation is using the 1.0 GeV mass sample at a reference mixing of 0.1, with the corresponding three dimensional histogram shown in Figure B.1. Both the nominal background expectation used to calculate the signal to square root of background ratio and the detector data can be seen in Figure 3.2.

Some low energy bins in the cascade like region have very low MC expectations (<1 event) and are therefore not taken into account in the analysis, to prevent unwanted behavior in the fit. Those are shown in dark green in the three dimensional histograms, and both background and data histograms show a strong decrease of events towards low energies in the cascade like bin. This background expectation is not necessarily supposed to agree with the data, because this is the distributions assuming nominal parameter values, before performing the fit to find the parameters that describe the data best. All parameters used in the analysis are discussed in Section 3.2.2, and post-fit data to MC comparisons are shown in Section 3.3.3.

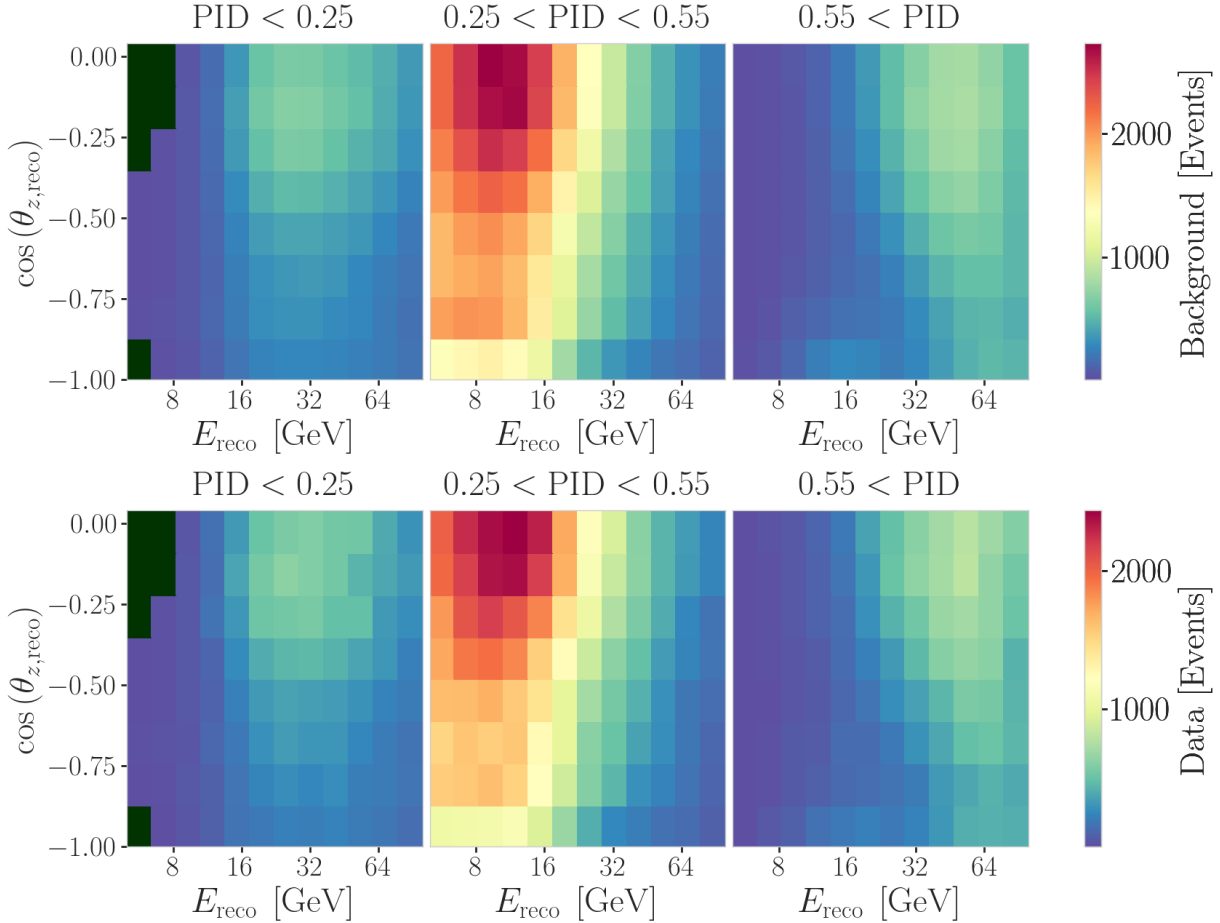


Figure 3.2: Background expectation in 9.28 years for all other parameters are at their nominal values (top) and observed data (bottom).

## 3.2 Statistical Analysis

### 3.2.1 Test Statistic

The measurements are performed by comparing the weighted MC to the data. Through variation of the nuisance and physics parameters that govern the weights, the best matching set of parameters can be found, by optimizing a fit metric. The comparison is done using a modified  $\chi^2$ , defined as

$$\chi_{\text{mod}}^2 = \sum_{i \in \text{bins}} \frac{(N_i^{\text{exp}} - N_i^{\text{obs}})^2}{N_i^{\text{exp}} + (\sigma_i^{\nu})^2 + (\sigma_i^{\mu})^2 + (\sigma_i^{\text{HNL}})^2} + \sum_{j \in \text{syst}} \frac{(s_j - \hat{s}_j)^2}{\sigma_{s_j}^2}, \quad (3.1)$$

as the fit metric. It is designed such that taking the difference between a free fit and a fit with fixed parameters based on a chosen hypothesis,  $\Delta\chi_{\text{mod}}^2$ , can directly be used as a *test statistic (TS)* for hypothesis testing, due to its asymptotic behavior. The total even expectation is  $N_i^{\text{exp}} = N_i^{\nu} + N_i^{\mu} + N_i^{\text{HNL}}$ , where  $N_i^{\nu}$ ,  $N_i^{\mu}$ , and  $N_i^{\text{HNL}}$  are the expected number of events in bin  $i$  from neutrinos, atmospheric muons, and HNLs, while  $N_i^{\text{obs}}$  is the observed number of events in the bin. The expected number of events from each particle type is calculated by summing the weights of all events in the bin  $N_i^{\text{type}} = \sum_i^{\text{type}} \omega_i$ , with the statistical uncertainty being  $(\sigma_i^{\text{type}})^2 = \sum_i^{\text{type}} \omega_i^2$ . The additional term in Equation 3.1 is included to apply a penalty term for

prior knowledge of the systematic uncertainties of the parameters where they are known.  $s_j$  are the systematic parameters that are varied in the fit, while  $\hat{s}_j$  are their nominal values and  $\sigma_{s_j}$  are the known uncertainties.

### 3.2.2 Physics Parameters

The variable physics parameter in this analysis is the mixing between the HNL and the SM  $\tau$  sector,  $|U_{\tau 4}|^2$ . It is varied continuously in the range of  $[0.0, 1.0]$  by applying the weighting scheme described in Section ???. The fit is initialized at an off-nominal value of 0.1. The other physics parameter, the mass  $m_4$  of the HNL, is implicitly fixed to one of the three discrete masses to be tested, by using the corresponding sample of the HNL simulation described in Section ??.

### 3.2.3 Nuisance Parameters

All systematic parameters introduced in Section ?? apart from the detector calibration uncertainties, are already parameterized in a continuous way and can be varied in the fit. To be able to do the same with the detector uncertainties, a novel method is applied that will briefly be introduced here before going into the selection of the free parameters.

#### Treatment of Detector Systematic Uncertainties

Since the variations related to the detector calibration uncertainties introduced in Section ?? are estimated by simulating MC at discrete values of the systematic parameters, a method to derive continuous variations is needed to perform the fit. The method applied here was initially introduced in [83] and first used in the low energy sterile neutrino search in [19] (section 7.4.3). Using a *likelihood-free inference* technique, re-weighting factors are found for every event in the nominal MC sample, given a specific choice of detector systematic parameters. These factors quantify how much more or less likely the event would be for the corresponding change in detector response from the nominal parameters. Without going into the details of the method, which were already exhaustively discussed in [83] and [19], the performance is assessed here for the HNL signal simulation. In order to do so, the weights are applied to the nominal MC samples, choosing the detector systematic values used to produce the discrete samples and the resulting event expectations are compared to the expectations from the individual, discrete MC samples. The bin counts are compared by calculating the pull defined as

$$p = \frac{N_{\text{reweighted}} - N_{\text{sys}}}{\sqrt{\sigma_{\text{reweighted}}^2 + \sigma_{\text{sys}}^2}}, \quad (3.2)$$

where  $N$  are the bin-wise event expectations and  $\sigma$  are their MC uncertainty. For the SM BG simulation, the performance was already investigated in [84] (section 7.4.4, appendix B5) and the re-weighted nominal MC was shown to be in agreement with the discrete systematic sets at a sufficient level. Figure ?? shows the bin-wise pulls for the 1.0 GeV HNL mass sample at a mixing of 0.1 for a selection of the discrete systematic samples, where the DOM efficiency and the bulk ice absorption was varied by  $\pm 10\%$ . As expected,

[83]: Fischer et al. (2023), “Treating detector systematics via a likelihood free inference method”

[19]: Trettin (2023), “Search for eV-scale sterile neutrinos with IceCube DeepCore”

[84]: Lohfink (2023), “Testing non-standard neutrino interaction parameters with IceCube-DeepCore”

add bin-wise pulls and pull distribution for selection of sets and rest to backup (RED)

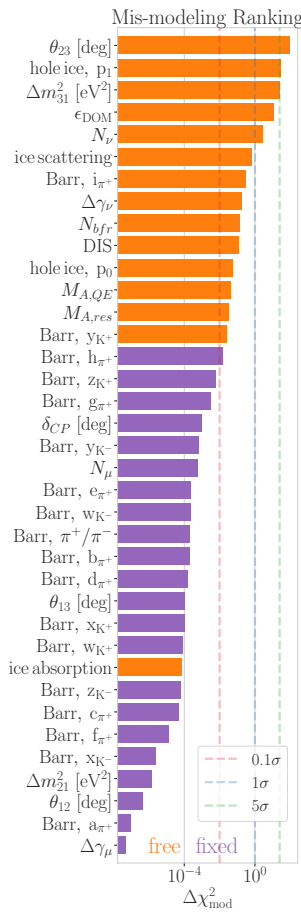


**Figure 3.3:** Mis-modeling impact ranking of the systematic parameters. The mis-modeling is calculated as the fit metric difference between a fit with the parameter fixed at its nominal value and a fit with the parameter pulled up by  $+1\sigma$ . The test was performed using Asimov data of the 1.0 GeV mass sample at a reference mixing of 0.1.

Need cite here! (RED)

the pull distributions follow a standard normal distribution, without strong clustering or any systematic deviations. The spread of the distribution is slightly smaller than 1.0 and the center is close to 0.0. A similar performance is found for the additional systematic variations and the detailed figures can be found in Section B.2.

## Free Parameters

To decide which systematic uncertainties should be included in the fit, we test the potential impact they have on the TS if they are neglected. The test is performed by creating Asimov data using the BG simulation and the HNL simulation of the 1.0 GeV mass sample at a mixing value of 0.1, which is chosen as a benchmark physics parameter, but the explicit choice does not have a significant impact on the test. The systematic parameter of interest is set to a value above its nominal expectation, either pulled up by  $+1\sigma$  or by an educated estimate for parameters without a well-defined uncertainty. A fit is performed fixing the systematic parameter of interest and leaving all additional parameters free. The resulting TS is the fit metric difference between this fit and a fit with all parameters free, which would result in a fit metric of 0.0 for this Asimov test. This difference is called mis-modelling significance and parameters below a significance of  $0.1\sigma$  are fixed. The test is performed in an iterative manner until the final set of free parameters is found.

Figure 3.3 shows the resulting significances of one of these tests. The parameters tested are the systematic parameters introduced in Section ?? and the atmospheric oscillation parameters mentioned in Section 3.1. In the final selection of free parameters the Barr  $h_{\pi^+}$  parameter was also left free, to sufficiently cover the relevant energy production range of the Pions, as can be seen in Figure ??, where both for Kaons and Pions the uncertainties are included for primary energies above 30 GeV and  $x_{\text{lab}} > 0.1$ . Additionally, the ice absorption is still kept free, despite showing a small significance, which is done because the bulk ice parameters are not well constrained and are known to have a large impact, which might be concealed in this idealized test, due to correlations with the other parameters. In this test, the effect of correlations is challenging to consider, because only the impact of one parameter is tested at a time, using the overall mis-modelling significance as a measure. The mis-modelling could be reduced by a correlated parameter capturing the effect of the parameter of interest. For this reason a very conservative threshold of  $0.1\sigma$  is chosen and some parameters below the threshold are still left free in the fit.

All nuisance parameters that are left free in the fit are summarized in Table 3.4, showing their nominal values, the allowed fit ranges, and their Gaussian prior, if applicable. The scaling parameter  $N_{\nu}$  is included to account for the overall normalization of the neutrino rate, and it has the identical effect on the SM neutrino events and the BSM HNL events, because they both originate from the same neutrino flux. Despite being known to  $\sim 5\%$  in this energy range, there is no prior applied to this parameter, because the fit itself is able to constrain it well, which can be seen by the large impact it shows in Figure 3.3. Concerning the atmospheric neutrino flux, the CR power law flux correction factor  $\Delta\gamma_{\nu}$  introduced in Section ?? is included with nominal value of 0.0 which corresponds to the baseline flux model by Honda *et al* [74]. A slightly conservative prior of 0.1 is applied to the

[74]: Honda et al. (2015), "Atmospheric neutrino flux calculation using the NRLMSISE-00 atmospheric model"

Parameter	Nominal	Range	Prior
$\theta_{23}[\circ]$	47.5047	[0.0, 90.0]	-
$\Delta m_{31}^2 [\text{eV}^2]$	0.002475	[0.001, 0.004]	-
$N_\nu$	1.0	[0.1, 2.0]	-
$\Delta\gamma_\nu$	0.0	[-0.5, 0.5]	0.1
Barr $h_{\pi^+}$	0.0	[-0.75, 0.75]	0.15
Barr $i_{\pi^+}$	0.0	[-3.05, 3.05]	0.61
Barr $y_{K^+}$	0.0	[-1.5, 1.5]	0.3
DIS	0.0	[-0.5, 1.5]	1.0
$M_{A,\text{QE}}$	0.0	[-2.0, 2.0]	1.0
$M_{A,\text{res}}$	0.0	[-2.0, 2.0]	1.0
$\epsilon_{\text{DOM}}$	1.0	[0.8, 1.2]	0.1
hole ice $p_0$	0.101569	[-0.6, 0.5]	-
hole ice $p_1$	-0.049344	[-0.2, 0.2]	-
bulk ice absorption	1.0	[0.85, 1.15]	-
bulk ice scattering	1.05	[0.9, 1.2]	-
$N_{\text{bfr}}$	0.0	[-0.2, 1.2]	-

parameter, while latest measurements show an uncertainty of 0.05 [85]. The Barr parameters are constrained by a Gaussian prior, taken from [86]. All the detector systematic uncertainties discussed in Section ?? are included in the fit. The DOM efficiency  $\epsilon_{\text{DOM}}$  is constrained by a Gaussian prior with a width of 0.1, which is a conservative estimate based on the studies of the optical efficiency using minimum ionizing muons from [87, 88]. The two atmospheric neutrino oscillation parameters  $\theta_{23}$  and  $\Delta m_{31}^2$  are also included in the fit with nominal values of  $47.5^\circ$  and  $2.48 \times 10^{-3} \text{ eV}^2$  [82], respectively. Since they govern the shape and the strength of the tau neutrino flux, by defining the oscillation from  $\nu_\mu$  to  $\nu_\tau$ , they are also relevant for the HNL signal shape.

### 3.2.4 Low Energy Analysis Framework

The analysis is performed using the PISA [89] [90] software framework, which was developed to perform analyses of small signals in high-statistics neutrino oscillation experiments. It is used to generate the expected event distributions from several MC samples, which can then be compared to the observed data. The expectation for each MC sample is calculated by applying physics and nuisance parameter effects in a stage-wise manner, before combining them to the final expectation.

## 3.3 Analysis Checks

Fitting to data is performed in a *blind* manner, where the analyzer does not immediately see the fitted physics and nuisance parameter values, but first checks that a set of pre-defined *goodness of fit* (*GOF*) criteria are fulfilled. This is done to circumvent the so-called *confirmation bias* [91], where the analyzer might be tempted to construct the analysis in a way that confirms their expectation. After the GOF criteria are met to satisfaction, the fit results are unblinded and the full result can be revealed. Before these blind fits to data are performed, the robustness of the analysis method is tested using pseudo-data that is generated from the MC.

**Table 3.4:** Systematic uncertainty parameters that are left free to float in the fit. Their allowed fit ranges are shown with the nominal value and the Gaussian prior width if applicable.

[85]: Evans et al. (2017), “Uncertainties in atmospheric muon-neutrino fluxes arising from cosmic-ray primaries”

[86]: Barr et al. (2006), “Uncertainties in Atmospheric Neutrino Fluxes”

[87]: Feintzeig (2014), “Searches for Point-like Sources of Astrophysical Neutrinos with the IceCube Neutrino Observatory”

[88]: Kulacz (2019), “In Situ Measurement of the IceCube DOM Efficiency Factor Using Atmospheric Minimum Ionizing Muons”

[82]: Yu et al. (2023), “Recent neutrino oscillation result with the IceCube experiment”

I could add some final level effects of some systematics on the 3D binning and maybe discuss how they are different from the signal shape, or so? (ORANGE)

[89]: Aartsen et al. (2020), “Computational techniques for the analysis of small signals in high-statistics neutrino oscillation experiments”

[91]: Nickerson (1998), “Confirmation Bias: A Ubiquitous Phenomenon in Many Guises”

### 3.3.1 Minimization Robustness

1: There is a degeneracy between the lower octant ( $\theta_{23} < 45^\circ$ ) and the upper octant ( $\theta_{23} > 45^\circ$ ), which can lead to fit metric minima (local and global) at two positions that are mirrored around  $45^\circ$  in  $\theta_{23}$ .

[92]: Dembinski et al. (2022), *scikit-hep/minuit*: v2.17.0

[93]: James et al. (1975), “Minuit: A System for Function Minimization and Analysis of the Parameter Errors and Correlations”

Fit	Err.	Prec.	Tol.
Coarse	1e-1	1e-8	1e-1
Fine	1e-5	1e-14	1e-5

**Table 3.5:** Migrad settings for the two stages in the minimization routine. *Err.* are the step size for the numerical gradient estimation, *Prec.* is the precision with which the LLH is calculated, and *Tol.* is the tolerance for the minimization.

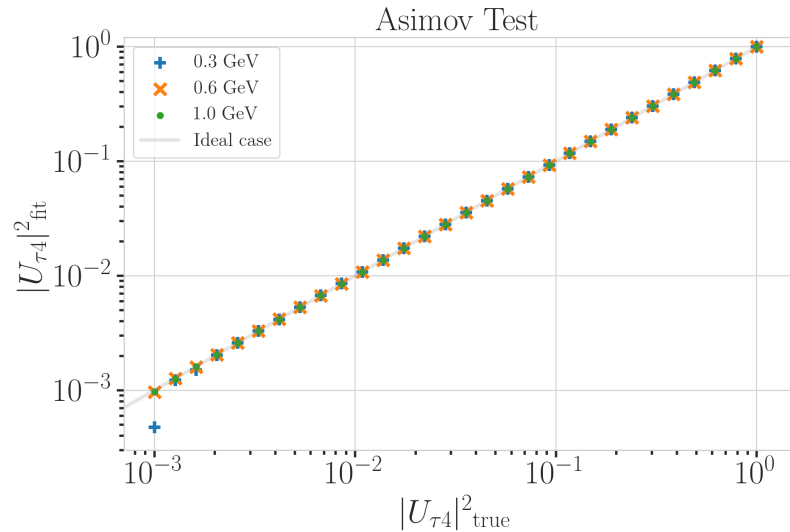
Find first occurance of "Asimov" and add reference and explain it there (RED)

2: A pseudo-data set without statistical fluctuations is called Asimov data set.

**Figure 3.4:** Asimov inject/recover test results for all three mass samples. Mixing values between  $10^{-3}$  and  $10^0$  are injected and fit back with the full analysis chain. The injected parameter is always recovered within the statistical uncertainty or at an insignificant fit metric difference.

To find the set of parameters that best describes the data, a staged minimization routine is used. In the first stage, a fit with coarse minimizer settings is performed to find a rough estimate of the *best fit point* (BFP). In the second stage, the fit is performed again in both octants<sup>1</sup> of  $\theta_{23}$ , starting from the BFP of the coarse fit. For each individual fit the *MIGRAD* routine of *iminuit* [92] is used to minimize the  $\chi^2_{\text{mod}}$  fit metric defined in Equation 3.1. *Iminuit* is a fast, python compatible minimizer based on the *Minuit2 C++ library* [93]. The individual minimizer settings for both stages are shown in Table 3.5.

To test the minimization routine and to make sure it consistently recovers any physics parameters, pseudo-data sets are produced from the MC by choosing the nominal nuisance parameters and specific physics parameters, without adding any statistical or systematic fluctuations to it. These so-called *Asimov*<sup>2</sup> data sets are then fit back with the full analysis chain. This type of test is called *Asimov inject/recover test*. A set of mixing values between  $10^{-3}$  and  $10^0$  is injected and fit back. Without fluctuations the fit is expected to always recover the injected parameters (both physics and nuisance parameters). The fitted mixing values from the Asimov inject/recover tests are compared to the true injected values in Figure 3.4 for all three mass samples. As desired, the fit is always able to recover the injected physics parameter and the nuisance parameters within the statistical uncertainty or at an insignificant fit metric difference.



### 3.3.2 Goodness of Fit

To estimate the GOF, pseudo-data is generated from the MC by injecting the BFP parameters as true parameters and then fluctuating the expected bin counts to account for MC uncertainty and Poisson fluctuations in data. First, the expectation value of each bin is drawn from a Gaussian distribution centered at the nominal expectation value with a standard deviation corresponding to the MC uncertainty of the bin. Based on this sampled expectation value, each bin count is drawn from a Poisson distribution, independently, to get the final pseudo-data set. These pseudo-data sets are

analyzed with the same analysis chain as the real data, resulting in a final fit metric value for each pseudo-data set. By comparing the distribution of fit metric values from this *ensemble* of pseudo-data trials to the fit metric of the fit to real data, a p-value can be calculated. The p-value is the probability of finding a value of the fit metric at least as large as the one from the data fit. Figure 3.5 shows the distribution from the ensemble tests for the 0.6 GeV mass sample and the observed value from the fit, resulting in a p-value of 28.5 %. The p-values for the 0.3 GeV and 1.0 GeV are 28.3 % and 26.0 %, respectively, and the corresponding plots are shown in Section ???. Based on this test, it is concluded that the fit result is compatible with the expectation from the ensemble of pseudo-data trials.

Add 3D BFP-data pull distribution for one mass (they look the same, no?) (RED)

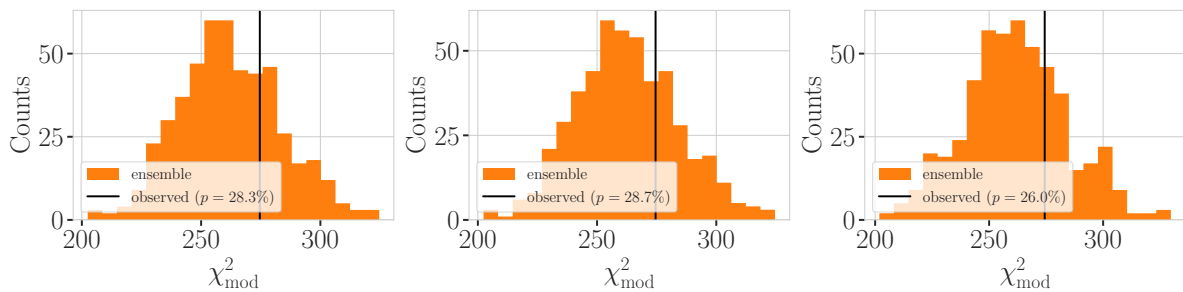


**Figure 3.5:** Observed fit metric (data fit) and fit metric distribution from pseudo-data ensemble generated around the best fit point. Shown are the results for all three mass samples, with the ensemble distribution on orange, the observed value in black, and the p-value in the legend.

### 3.3.3 Data/MC Agreement

At the BFP, the agreement between the data and simulation is probed by comparing the one dimensional analysis distributions for PID, energy, and cosine of the zenith angle. As an example, two distributions for the 0.6 GeV mass sample are shown in Figure ???. The data is compared to the total MC expectation, which is also split up into the individual signal and background components for illustration. Good agreement can be observed in the pull distributions, and is quantified by a reduced  $\chi^2$ , which is close to 1.0 for all distributions. The reduced  $\chi^2$  for all investigated distributions is listed in Table ???, while the distributions themselves can be found in Section ???.

specify which they are, once I have them (RED)

add 1-d data/mc agreement for example mass sample (0.6?) and all 3 analysis variables (RED)

add table with reduced chi2 for all 1-d distributions (RED)

## 3.4 Results

### 3.4.1 Best Fit Nuisance Parameters

The resulting nuisance parameter values from the fits are illustrated in Figure 3.6, where the differences to the nominal values are shown, normalized by the distance to the closest boundary. The results from all three fits are shown in the same plot and the fits prefer values of the same size for all three mass samples. For parameters that have a Gaussian prior, the  $1\sigma$  range is also displayed. As was already confirmed during the blind fit procedure, all fitted parameters are within this range. The effective ice model parameter,  $N_{\text{bf}}$ , prefers a value of  $\sim 0.74$ , indicating that the data fits better to an ice model that includes real birefringence effects. For completeness, the explicit results are listed in Table B.1. There, the nominal values and the absolute differences to the best fit value are also presented.

Cite (again)! (RED)

Show best fit hole ice angular acceptance compared to nominal and flasher/in-situ fits, maybe? (YELLOW)

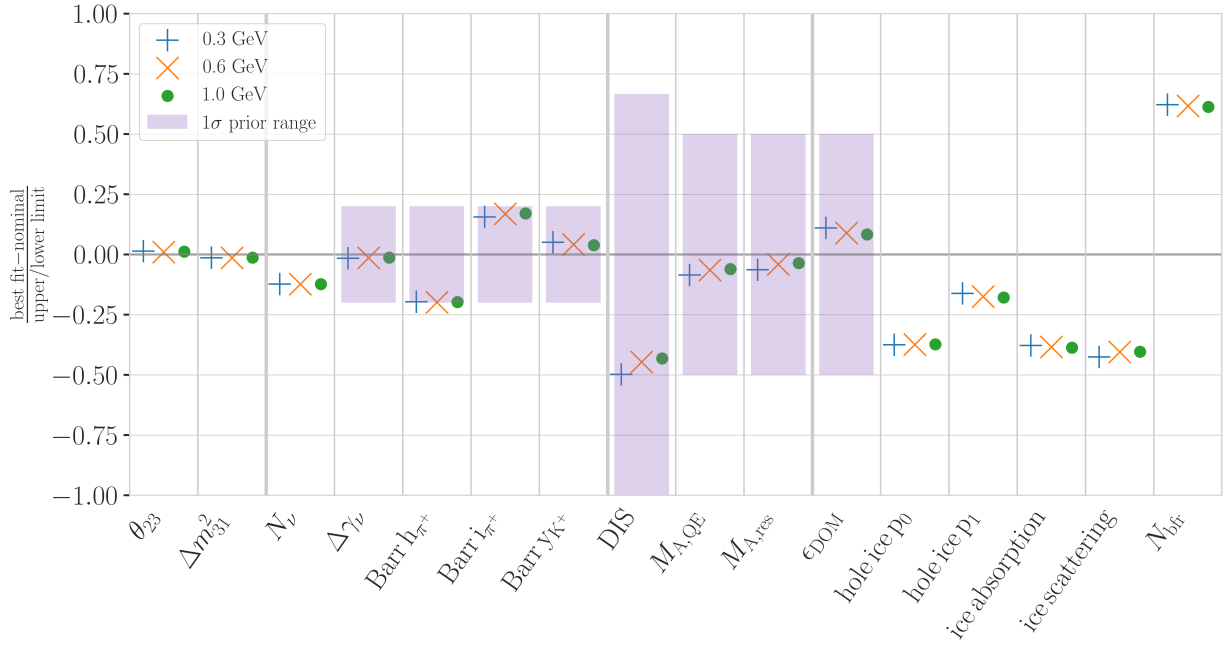


**Figure 3.6:** Best fit nuisance parameter distances to the nominal values, normalized by the distance to the closest boundary. For parameters with a Gaussian prior, the  $+1\sigma$  range is also shown.

### 3.4.2 Best Fit Parameters and Limits

The fitted mixing values are

$$\begin{aligned} |U_{\tau 4}|^2(0.3 \text{ GeV}) &= 0.003^{+0.084}, \\ |U_{\tau 4}|^2(0.6 \text{ GeV}) &= 0.080^{+0.134}, \text{ and} \\ |U_{\tau 4}|^2(1.0 \text{ GeV}) &= 0.106^{+0.132}, \end{aligned}$$

with their  $+1\sigma$  uncertainty. All of them are compatible with the null hypothesis of 0.0 mixing, although the 0.6 GeV and 1.0 GeV fits indicate a mixing value of 0.08 and 0.106, respectively. The best fit mixing values and the corresponding upper limits at 68 % and 90 % confidence level (CL) are listed in Table 3.6, also showing the  $p$ -value to reject the null hypothesis. The CLs and  $p$ -value are estimated by assuming that *Wilks' theorem* [94] holds, meaning that the TS follows a  $\chi^2$  distribution with one degree of freedom.

[94]: Wilks (1938), “The Large-Sample Distribution of the Likelihood Ratio for Testing Composite Hypotheses”

**Table 3.6:** Best fit mixing values and the corresponding upper limits at 68 % and 90 % confidence level, as well as the  $p$ -value to reject the null hypothesis, estimated by assuming that Wilks' theorem holds.

HNL mass	$ U_{\tau 4} ^2$	68 % CL	90 % CL	NH $p$ -value
0.3 GeV	0.003	0.09	0.19	0.97
0.6 GeV	0.080	0.21	0.36	0.79
1.0 GeV	0.106	0.24	0.40	0.63

Figure 3.7 shows the observed TS profiles as a function of  $|U_{\tau 4}|^2$  for all three fits. The TS profile is the difference in  $\chi^2_{\text{mod}}$  between the free fit and a fit where the mixing is fixed to a specific value. Also shown is the expected TS profile, based on 100 pseudo-data trials, produced at the BFP and then fluctuated using both Poisson and Gaussian fluctuations, to include the data and the MC uncertainty as was explained in Section 3.3.2. The Asimov expectation and the 68 % and 90 % bands are shown and the observed TS profiles lie within the 68 % band for all three, confirming that they are compatible with statistical fluctuations of the observed data. For the 0.3 GeV fit, the observed contour is slightly tighter than the Asimov expectation, meaning that the

observed upper limits in  $|U_{\tau 4}|^2$  are slightly stronger than expected. For the 0.6 GeV the opposite is the case and the observed upper limit is therefore slightly weaker than expected. For the 1.0 GeV fit, the observed upper limit is very close to the Asimov expectation in the region where the 68 % and 90 % CLs thresholds are crossed. The observed upper limits are also shown in Table 3.6.

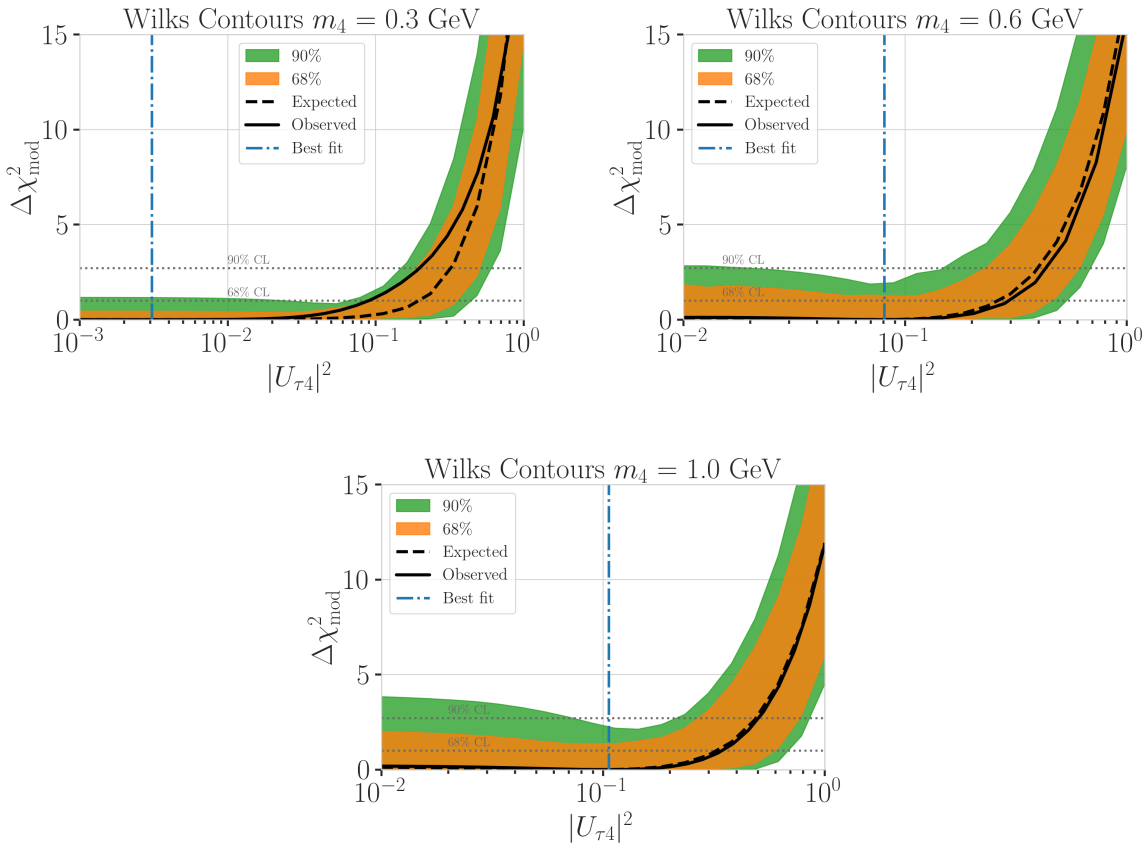


**Figure 3.7:** Best fit point TS profiles as a function of  $|U_{\tau 4}|^2$  for the 0.3 GeV, 0.6 GeV, and 1.0 GeV mass samples. Shown are the observed profiles, the Asimov expectation at the best fit point, and the 68 % and 90 % bands, based on 100 pseudo-data trials. Also indicated are the 68 % and 90 % CL levels assuming Wilks' theorem.

### 3.4.3 Agreement with Standard Model Three-Flavor Oscillation Measurement

### 3.4.4 Comparison to Other Experiments

## 3.5 Outlook

### 3.5.1 Shape Analysis Improvements

- ▶ estimate full contribution from cascade only events (underestimated due to limited sampling distributions)
- ▶ include double cascade classifier into Binning

Compare here the best fit oscillation parameters to the FLERCNN results and try to quantify it, stating the pitfalls of the comparisons (statistically fully dependent) (RED)

make summary plot (masses and mixing limits on one) and then discuss wrt to other experiments? (RED)

- ▶ further optimize binning

### 3.5.2 Test Coupling to Electron/Muon Flavor

### 3.5.3 Test Additional Coupling Processes

### 3.5.4 IceCube Upgrade

# Conclusion

# 4

Write conclusion (RED)

what was done?

1. set up model dependent and independent signal simulation for low energy double cascade events from HNL production and decay inside IceCube DeepCore
2. estimate performance of reconstructing and identifying these events
3. search for (cascade-like) events in 10 years of IceCube DeepCore data



## **APPENDIX**



# A

## Heavy Neutral Lepton Signal Simulation

### A.1 Model Independent Simulation Distributions

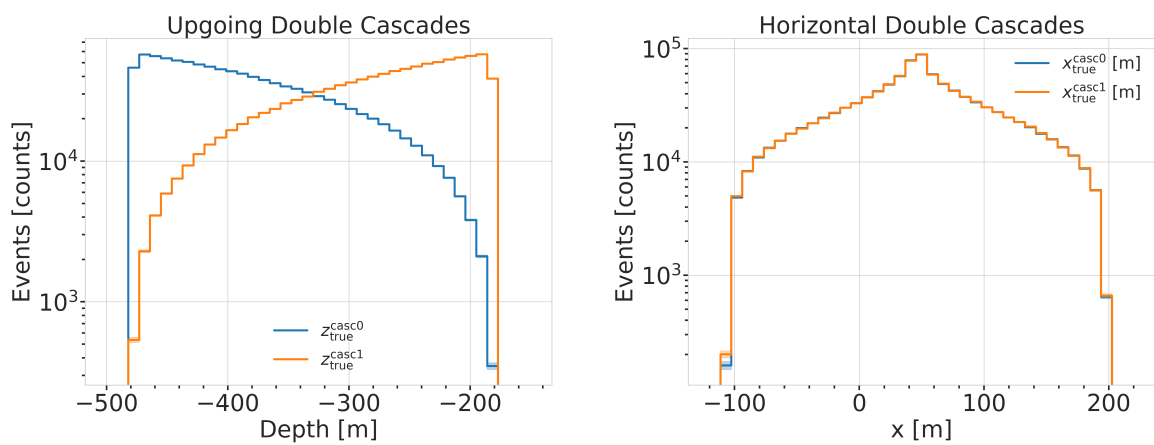


**Figure A.1:** Generation level distributions of the simplistic simulation sets. Vertical positions (left) and horizontal positions (right) of both sets are shown.

- Re-make plot with  $x, y$  for horizontal set one plot!
- Re-make plot with  $x, y, z$  for both cascades in one.
- Re-arrange plots in a more sensible way.

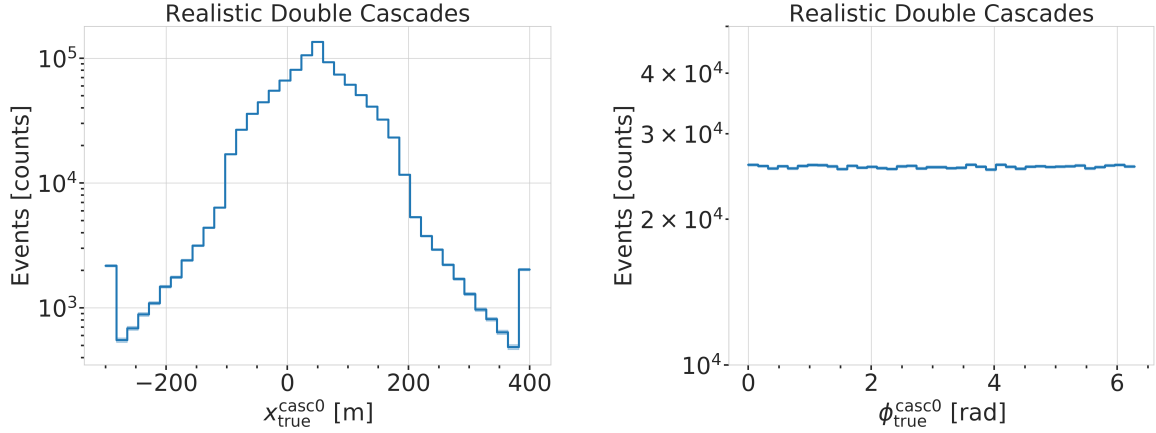


**Figure A.2:** Generation level distributions of the realistic simulation set. Shown are the cascade  $x, y, z$  positions (left) and direction angles (right).

## A.2 Model Dependent Simulation Distributions

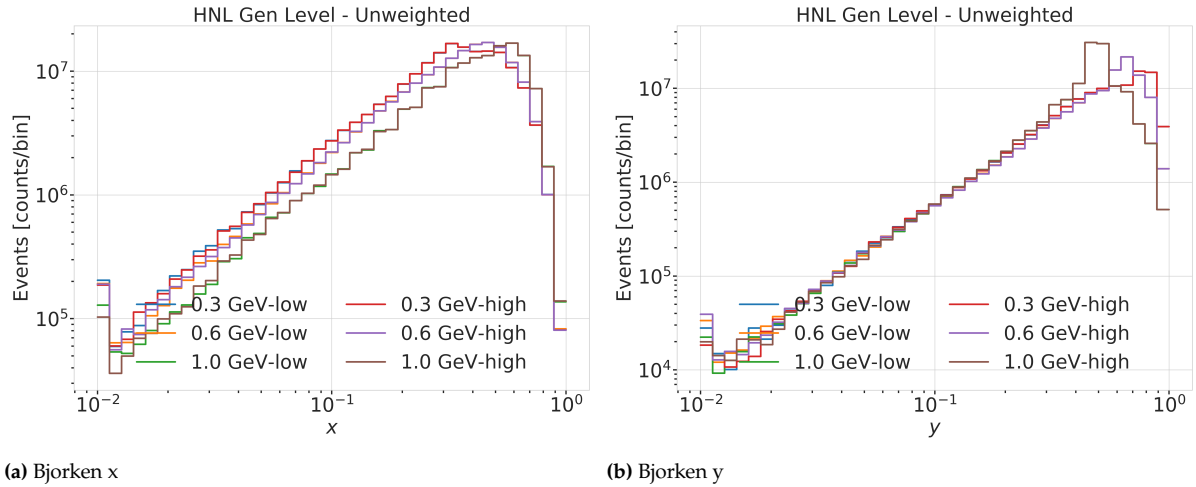


**Figure A.3:** Generation level distributions of the model dependent simulation.

# B

---

## Analysis Results

---

### B.1 Final Level Simulation Distributions

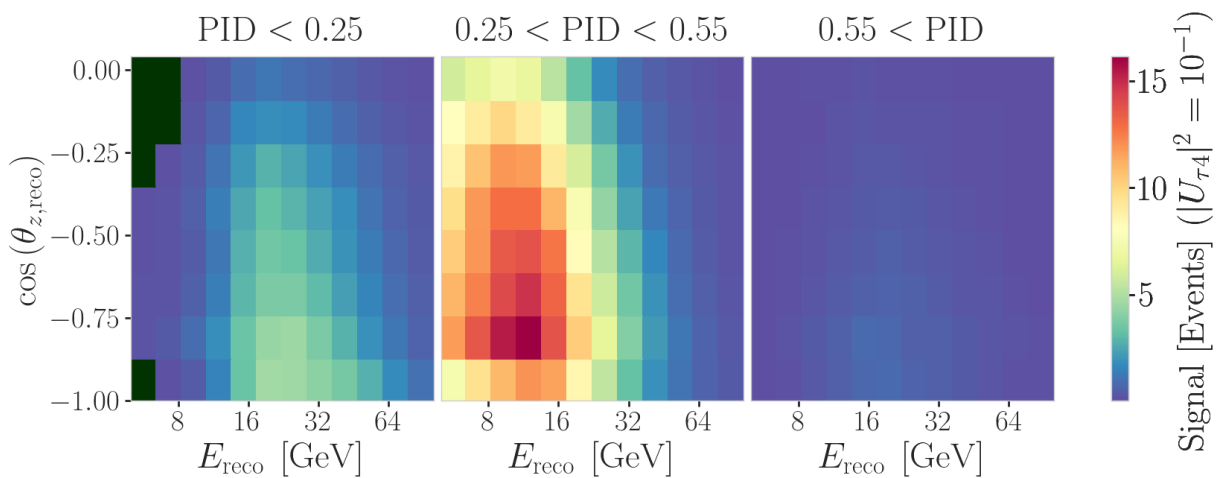


**Figure B.1:** Signal expectation in 9.28 years for the 1.0 GeV mass sample at a mixing of 0.1, while all other parameters are at their nominal values (top) and observed data (bottom).

### B.2 Treatment of Detector Systematic Uncertainties

### B.3 Best Fit Nuisance Parameters

fix design + significant digits to show (OR-ANGE)  
maybe show range/prior and then deviation in sigma, or absolute for the ones without prior

**Table B.1:** Best fit nuisance parameters for the three mass samples. Also shown is the nominal value and the difference between the nominal and the best fit.

Parameter	Nominal	Best Fit			Nominal - Best Fit		
		0.3 GeV	0.6 GeV	1.0 GeV	0.3 GeV	0.6 GeV	1.0 GeV
$ U_{\tau 4} ^2$	-	0.003019	0.080494	0.106141	-	-	-
$\theta_{23}[\circ]$	47.5047	48.117185	47.918758	48.010986	-0.612485	-0.414058	-0.506286
$\Delta m_{31}^2 [\text{eV}^2]$	0.002475	0.002454	0.002454	0.002455	0.000020	0.000021	0.000019
$N_\nu$	1.0	0.889149	0.889055	0.889559	0.110851	0.110945	0.110441
$\Delta \gamma_\nu$	0.0	-0.007926	-0.006692	-0.006596	0.007926	0.006692	0.006596
Barr $h_{\pi^+}$	0.0	-0.147475	-0.148481	-0.148059	0.147475	0.148481	0.148059
Barr $i_{\pi^+}$	0.0	0.475448	0.513393	0.521626	-0.475448	-0.513393	-0.521626
Barr $y_{K^+}$	0.0	0.076176	0.062893	0.057548	-0.076176	-0.062893	-0.057548
DIS	0.0	-0.248709	-0.223302	-0.215666	0.248709	0.223302	0.215666
$M_{A,\text{QE}}$	0.0	-0.170528	-0.128150	-0.120345	0.170528	0.128150	0.120345
$M_{A,\text{res}}$	0.0	-0.125855	-0.080875	-0.070716	0.125855	0.080875	0.070716
$\epsilon_{\text{DOM}}$	1.0	1.021984	1.017789	1.016689	-0.021984	-0.017789	-0.016689
hole ice $p_0$	0.101569	-0.161341	-0.161051	-0.160129	0.262910	0.262620	0.261698
hole ice $p_1$	-0.049344	-0.073701	-0.075596	-0.076261	0.024357	0.026252	0.026917
ice absorption	1.00	0.943261	0.942463	0.942000	0.056739	0.057537	0.058000
ice scattering	1.05	0.986152	0.989289	0.989438	0.063848	0.060711	0.060562
$N_{\text{bfr}}$	0.0	0.746684	0.740255	0.736215	-0.746684	-0.740255	-0.736215

# List of Figures

2.1	Feynman diagrams of neutrino weak interactions . . . . .	5
2.2	Current leading $ U_{e4}^2  - m_4$ limits . . . . .	9
2.3	Current leading $ U_{\mu 4}^2  - m_4$ limits . . . . .	10
2.4	Current leading $ U_{\tau 4}^2  - m_4$ limits . . . . .	11
2.5	Atmospheric neutrino fluxes . . . . .	13
2.6	Neutrino-nucleon deep inelastic scattering . . . . .	16
2.7	Total inclusive neutrino-nucleon cross-sections . . . . .	17
2.8	Feynman diagram of heavy neutral lepton production . . . . .	17
2.9	HNL decay widths . . . . .	18
2.10	Feynman diagram of heavy neutral lepton decay . . . . .	18
2.11	Theoretical mean HNL decay length (0.6 GeV mass) . . . . .	19
3.1	Three dimensional signal over square root of background expectation . . . . .	23
3.2	Three dimensional background expectation and observed data . . . . .	24
3.3	Nuisance parameter mis-modeling impact ranking . . . . .	26
3.4	Asimov inject/recover test . . . . .	28
3.5	Pseudo-data trials fit metric distributions . . . . .	29
3.6	Best fit nuisance parameter distances to nominal . . . . .	30
3.7	Best fit point TS profiles . . . . .	31
A.1	Simplified model independent simulation generation level distributions . . . . .	37
A.2	Realistic model independent simulation generation level distributions . . . . .	38
A.3	Model dependent simulation generation level distributions . . . . .	38
B.1	Three dimensional signal expectation . . . . .	39



# List of Tables

2.1 Standard model fermions . . . . .	4
2.2 Global fit neutrino mixing parameter results . . . . .	15
3.1 Final level background event/rate expectation . . . . .	22
3.2 Final level signal event/rate expectation . . . . .	22
3.3 Analysis binning . . . . .	22
3.4 Nuisance parameter nominal values and fit ranges . . . . .	27
3.5 Staged minimization routine settings . . . . .	28
3.6 Best fit mixing values and confidence limits . . . . .	30
B.1 Best fit nuisance parameters values . . . . .	40



# Bibliography

Here are the references in citation order.

- [1] W. Pauli. "Dear radioactive ladies and gentlemen". In: *Phys. Today* 31N9 (1978), p. 27 (cited on page 1).
- [2] C. L. Cowan et al. "Detection of the Free Neutrino: a Confirmation". In: *Science* 124.3212 (1956), pp. 103–104. doi: [10.1126/science.124.3212.103](https://doi.org/10.1126/science.124.3212.103) (cited on page 1).
- [3] G. Danby et al. "Observation of High-Energy Neutrino Reactions and the Existence of Two Kinds of Neutrinos". In: *Phys. Rev. Lett.* 9 (1 July 1962), pp. 36–44. doi: [10.1103/PhysRevLett.9.36](https://doi.org/10.1103/PhysRevLett.9.36) (cited on page 1).
- [4] K. Kodama et al. "Observation of tau neutrino interactions". In: *Physics Letters B* 504.3 (2001), pp. 218–224. doi: [https://doi.org/10.1016/S0370-2693\(01\)00307-0](https://doi.org/10.1016/S0370-2693(01)00307-0) (cited on page 1).
- [5] R. Davis, D. S. Harmer, and K. C. Hoffman. "Search for Neutrinos from the Sun". In: *Phys. Rev. Lett.* 20 (21 May 1968), pp. 1205–1209. doi: [10.1103/PhysRevLett.20.1205](https://doi.org/10.1103/PhysRevLett.20.1205) (cited on pages 1, 6).
- [6] M. G. Aartsen et al. "The IceCube Neutrino Observatory: instrumentation and online systems". In: *Journal of Instrumentation* 12.3 (Mar. 2017), P03012. doi: [10.1088/1748-0221/12/03/P03012](https://doi.org/10.1088/1748-0221/12/03/P03012) (cited on page 1).
- [7] C. N. Yang and R. L. Mills. "Conservation of Isotopic Spin and Isotopic Gauge Invariance". In: *Physical Review* 96.1 (Oct. 1954), pp. 191–195. doi: [10.1103/PhysRev.96.191](https://doi.org/10.1103/PhysRev.96.191) (cited on page 3).
- [8] S. Weinberg. "A Model of Leptons". In: *Phys. Rev. Lett.* 19 (21 Nov. 1967), pp. 1264–1266. doi: [10.1103/PhysRevLett.19.1264](https://doi.org/10.1103/PhysRevLett.19.1264) (cited on page 3).
- [9] S. L. Glashow. "Partial-symmetries of weak interactions". In: *Nuclear Physics* 22.4 (Feb. 1961), pp. 579–588. doi: [10.1016/0029-5582\(61\)90469-2](https://doi.org/10.1016/0029-5582(61)90469-2) (cited on page 3).
- [10] R. Jackiw. "Physical Formulations: Elementary Particle Theory. Relativistic Groups and Analyticity. Proceedings of the eighth Nobel Symposium, Aspenäsgården, Lerum, Sweden, May 1968. Nils Svartholm, Ed. Interscience (Wiley), New York, and Almqvist and Wiksell, Stockholm, 1969. 400 pp., illus. \$31.75." In: *Science* 168.3936 (1970), pp. 1196–1197. doi: [10.1126/science.168.3936.1196.b](https://doi.org/10.1126/science.168.3936.1196.b) (cited on page 3).
- [11] P. Higgs. "Broken symmetries, massless particles and gauge fields". In: *Physics Letters* 12.2 (1964), pp. 132–133. doi: [https://doi.org/10.1016/0031-9163\(64\)91136-9](https://doi.org/10.1016/0031-9163(64)91136-9) (cited on page 3).
- [12] S. Chatrchyan et al. "Observation of a New Boson at a Mass of 125 GeV with the CMS Experiment at the LHC". In: *Phys. Lett. B* 716 (2012), pp. 30–61. doi: [10.1016/j.physletb.2012.08.021](https://doi.org/10.1016/j.physletb.2012.08.021) (cited on page 3).
- [13] G. Aad et al. "Observation of a new particle in the search for the Standard Model Higgs boson with the ATLAS detector at the LHC". In: *Phys. Lett. B* 716 (2012), pp. 1–29. doi: [10.1016/j.physletb.2012.08.020](https://doi.org/10.1016/j.physletb.2012.08.020) (cited on page 3).
- [14] M. Gell-Mann. "A Schematic Model of Baryons and Mesons". In: *Resonance* 24 (1964), pp. 923–925 (cited on page 3).
- [15] G. Zweig. "An SU(3) model for strong interaction symmetry and its breaking. Version 2". In: *DEVELOPMENTS IN THE QUARK THEORY OF HADRONS. VOL. 1. 1964 - 1978*. Ed. by D. B. Lichtenberg and S. P. Rosen. Feb. 1964, pp. 22–101 (cited on page 3).
- [16] D. J. Gross and F. Wilczek. "Ultraviolet Behavior of Non-Abelian Gauge Theories". In: *PRL* 30.26 (June 1973), pp. 1343–1346. doi: [10.1103/PhysRevLett.30.1343](https://doi.org/10.1103/PhysRevLett.30.1343) (cited on page 3).
- [17] C. Giunti and C. W. Kim. *Fundamentals of Neutrino Physics and Astrophysics*. Oxford University Press, Mar. 2007 (cited on page 3).

- [18] M. D. Schwartz. *Quantum Field Theory and the Standard Model*. Cambridge University Press, 2013 (cited on page 3).
- [19] A. Trettin. "Search for eV-scale sterile neutrinos with IceCube DeepCore". PhD thesis. Berlin, Germany: Humboldt-Universität zu Berlin, Mathematisch-Naturwissenschaftliche Fakultät, 2023. doi: <https://github.com/atrettin/PhD-Thesis> (cited on pages 5, 8, 25).
- [20] N. Deruelle, J.-P. Uzan, and P. de Forcrand-Millard. *Relativity in Modern Physics*. Oxford University Press, Aug. 2018 (cited on page 6).
- [21] R. L. Workman et al. "Review of Particle Physics". In: *Progress of Theoretical and Experimental Physics* 2022.8 (Aug. 2022), p. 083C01. doi: [10.1093/ptep/ptac097](https://doi.org/10.1093/ptep/ptac097) (cited on page 6).
- [22] M. Fukugita and T. Yanagida. "Baryogenesis without grand unification". In: *Physics Letters B* 174.1 (1986), pp. 45–47. doi: [https://doi.org/10.1016/0370-2693\(86\)91126-3](https://doi.org/10.1016/0370-2693(86)91126-3) (cited on page 6).
- [23] Y. Fukuda et al. "Evidence for Oscillation of Atmospheric Neutrinos". In: *Phys. Rev. Lett.* 81 (8 Aug. 1998), pp. 1562–1567. doi: [10.1103/PhysRevLett.81.1562](https://doi.org/10.1103/PhysRevLett.81.1562) (cited on page 6).
- [24] Q. R. Ahmad and other. "Direct Evidence for Neutrino Flavor Transformation from Neutral-Current Interactions in the Sudbury Neutrino Observatory". In: *Phys. Rev. Lett.* 89 (1 June 2002), p. 011301. doi: [10.1103/PhysRevLett.89.011301](https://doi.org/10.1103/PhysRevLett.89.011301) (cited on page 6).
- [25] S. Alam et al. "Completed SDSS-IV extended Baryon Oscillation Spectroscopic Survey: Cosmological implications from two decades of spectroscopic surveys at the Apache Point Observatory". In: *Phys. Rev. D* 103 (8 Apr. 2021), p. 083533. doi: [10.1103/PhysRevD.103.083533](https://doi.org/10.1103/PhysRevD.103.083533) (cited on page 6).
- [26] N. Aghanim et al. "Planck2018 results: VI. Cosmological parameters". In: *Astronomy & Astrophysics* 641 (Sept. 2020), A6. doi: [10.1051/0004-6361/201833910](https://doi.org/10.1051/0004-6361/201833910) (cited on page 6).
- [27] M. Aker et al. "Direct neutrino-mass measurement with sub-electronvolt sensitivity". In: *Nature Phys.* 18.2 (2022), pp. 160–166. doi: [10.1038/s41567-021-01463-1](https://doi.org/10.1038/s41567-021-01463-1) (cited on page 6).
- [28] T. Asaka, S. Blanchet, and M. Shaposhnikov. "The nuMSM, dark matter and neutrino masses". In: *Phys. Lett. B* 631 (2005), pp. 151–156. doi: [10.1016/j.physletb.2005.09.070](https://doi.org/10.1016/j.physletb.2005.09.070) (cited on page 8).
- [29] T. Asaka and M. Shaposhnikov. "The νMSM, dark matter and baryon asymmetry of the universe". In: *Phys. Lett. B* 620 (2005), pp. 17–26. doi: [10.1016/j.physletb.2005.06.020](https://doi.org/10.1016/j.physletb.2005.06.020) (cited on page 8).
- [30] P. Minkowski. " $\mu \rightarrow e \gamma$  at a rate of one out of  $10^9$  muon decays?" In: *Physics Letters B* 67.4 (Apr. 1977), pp. 421–428. doi: [10.1016/0370-2693\(77\)90435-X](https://doi.org/10.1016/0370-2693(77)90435-X) (cited on page 8).
- [31] T. Yanagida. "Horizontal Symmetry and Masses of Neutrinos". In: *Progress of Theoretical Physics* 64.3 (Sept. 1980), pp. 1103–1105. doi: [10.1143/PTP.64.1103](https://doi.org/10.1143/PTP.64.1103) (cited on page 8).
- [32] S. L. Glashow. "The Future of Elementary Particle Physics". In: *NATO Sci. Ser. B* 61 (1980), p. 687. doi: [10.1007/978-1-4684-7197-7\\_15](https://doi.org/10.1007/978-1-4684-7197-7_15) (cited on page 8).
- [33] M. Gell-Mann, P. Ramond, and R. Slansky. "Complex Spinors and Unified Theories". In: *Conf. Proc. C* 790927 (1979), pp. 315–321 (cited on page 8).
- [34] R. N. Mohapatra and G. Senjanović. "Neutrino Mass and Spontaneous Parity Nonconservation". In: *Phys. Rev. Lett.* 44 (14 Apr. 1980), pp. 912–915. doi: [10.1103/PhysRevLett.44.912](https://doi.org/10.1103/PhysRevLett.44.912) (cited on page 8).
- [35] M. G. Aartsen et al. "eV-Scale Sterile Neutrino Search Using Eight Years of Atmospheric Muon Neutrino Data from the IceCube Neutrino Observatory". In: *Phys. Rev. Lett.* 125.14 (2020), p. 141801. doi: [10.1103/PhysRevLett.125.141801](https://doi.org/10.1103/PhysRevLett.125.141801) (cited on page 8).
- [36] J.-L. Tastet, O. Ruchayskiy, and I. Timiryasov. "Reinterpreting the ATLAS bounds on heavy neutral leptons in a realistic neutrino oscillation model". In: *JHEP* 12 (2021), p. 182. doi: [10.1007/JHEP12\(2021\)182](https://doi.org/10.1007/JHEP12(2021)182) (cited on page 8).
- [37] D. A. Bryman and R. Shrock. "Constraints on Sterile Neutrinos in the MeV to GeV Mass Range". In: *Phys. Rev. D* 100 (2019), p. 073011. doi: [10.1103/PhysRevD.100.073011](https://doi.org/10.1103/PhysRevD.100.073011) (cited on pages 9, 10).
- [38] A. Aguilar-Arevalo et al. "Improved search for heavy neutrinos in the decay  $\pi \rightarrow ev$ ". In: *Phys. Rev. D* 97.7 (2018), p. 072012. doi: [10.1103/PhysRevD.97.072012](https://doi.org/10.1103/PhysRevD.97.072012) (cited on page 9).

- [39] G. Bellini et al. "New limits on heavy sterile neutrino mixing in B8 decay obtained with the Borexino detector". In: *Phys. Rev. D* 88.7 (2013), p. 072010. doi: [10.1103/PhysRevD.88.072010](https://doi.org/10.1103/PhysRevD.88.072010) (cited on pages 9, 12).
- [40] D. Britton et al. "Improved search for massive neutrinos in  $\pi^+ \rightarrow e^+ \nu$  decay". In: *Physical Review D* 46 (1992) (cited on page 9).
- [41] C. J. Parkinson et al. "Search for heavy neutral lepton production at the NA62 experiment". In: *PoS EPS-HEP2021* (2022), p. 686. doi: [10.22323/1.398.0686](https://doi.org/10.22323/1.398.0686) (cited on pages 9, 10).
- [42] K. Abe et al. "Search for heavy neutrinos with the T2K near detector ND280". In: *Phys. Rev. D* 100.5 (2019), p. 052006. doi: [10.1103/PhysRevD.100.052006](https://doi.org/10.1103/PhysRevD.100.052006) (cited on pages 9, 10).
- [43] P. Abreu et al. "Search for neutral heavy leptons produced in Z decays". In: *Z. Phys. C* 74 (1997). [Erratum: *Z.Phys.C* 75, 580 (1997)], pp. 57–71. doi: [10.1007/s002880050370](https://doi.org/10.1007/s002880050370) (cited on pages 9, 11).
- [44] R. Barouki, G. Marocco, and S. Sarkar. "Blast from the past II: Constraints on heavy neutral leptons from the BEBC WA66 beam dump experiment". In: *SciPost Phys.* 13 (2022), p. 118. doi: [10.21468/SciPostPhys.13.5.118](https://doi.org/10.21468/SciPostPhys.13.5.118) (cited on pages 9–11).
- [45] F. Bergsma et al. "A Search for Decays of Heavy Neutrinos". In: *Phys. Lett. B* 128 (1983). Ed. by J. Tran Thanh Van, p. 361. doi: [10.1016/0370-2693\(83\)90275-7](https://doi.org/10.1016/0370-2693(83)90275-7) (cited on page 9).
- [46] G. Aad et al. "Search for heavy neutral leptons in decays of W bosons produced in 13 TeV  $pp$  collisions using prompt and displaced signatures with the ATLAS detector". In: *JHEP* 10 (2019), p. 265. doi: [10.1007/JHEP10\(2019\)265](https://doi.org/10.1007/JHEP10(2019)265) (cited on pages 9, 10).
- [47] G. Aad et al. "Search for Heavy Neutral Leptons in Decays of W Bosons Using a Dilepton Displaced Vertex in  $\sqrt{s} = 13\text{TeV}$   $pp$  Collisions with the ATLAS Detector". In: *Phys. Rev. Lett.* 131 (6 Aug. 2023), p. 061803. doi: [10.1103/PhysRevLett.131.061803](https://doi.org/10.1103/PhysRevLett.131.061803) (cited on pages 9, 10).
- [48] A. M. Sirunyan et al. "Search for heavy neutral leptons in events with three charged leptons in proton-proton collisions at  $\sqrt{s} = 13\text{ TeV}$ ". In: *Phys. Rev. Lett.* 120.22 (2018), p. 221801. doi: [10.1103/PhysRevLett.120.221801](https://doi.org/10.1103/PhysRevLett.120.221801) (cited on pages 9, 10).
- [49] A. Tumasyan et al. "Search for long-lived heavy neutral leptons with displaced vertices in proton-proton collisions at  $\sqrt{s} = 13\text{ TeV}$ ". In: *JHEP* 07 (2022), p. 081. doi: [10.1007/JHEP07\(2022\)081](https://doi.org/10.1007/JHEP07(2022)081) (cited on pages 9, 10).
- [50] A. Vaitaitis et al. "Search for neutral heavy leptons in a high-energy neutrino beam". In: *Phys. Rev. Lett.* 83 (1999), pp. 4943–4946. doi: [10.1103/PhysRevLett.83.4943](https://doi.org/10.1103/PhysRevLett.83.4943) (cited on pages 9, 10).
- [51] E. Fernandez-Martinez et al. "Effective portals to heavy neutral leptons". In: *JHEP* 09 (2023), p. 001. doi: [10.1007/JHEP09\(2023\)001](https://doi.org/10.1007/JHEP09(2023)001) (cited on pages 9–11).
- [52] G. Bernardi et al. "Search for Neutrino Decay". In: *Phys. Lett. B* 166 (1986), pp. 479–483. doi: [10.1016/0370-2693\(86\)91602-3](https://doi.org/10.1016/0370-2693(86)91602-3) (cited on page 9).
- [53] S. Ito et al. "Search for heavy neutrinos in  $\pi^+ \rightarrow \mu^+\nu$  decay and status of lepton universality test in the PIENU experiment". In: *JPS Conf. Proc.* 33 (2021). Ed. by N. Saito, pp. 011131-1–011131-6. doi: [10.7566/JPSCP.33.011131](https://doi.org/10.7566/JPSCP.33.011131) (cited on page 9).
- [54] P. Abratenko et al. "Search for Heavy Neutral Leptons in Electron-Positron and Neutral-Pion Final States with the MicroBooNE Detector". In: *Phys. Rev. Lett.* 132.4 (2024), p. 041801. doi: [10.1103/PhysRevLett.132.041801](https://doi.org/10.1103/PhysRevLett.132.041801) (cited on pages 9, 10).
- [55] P. Astier et al. "Search for heavy neutrinos mixing with tau neutrinos". In: *Phys. Lett. B* 506 (2001), pp. 27–38. doi: [10.1016/S0370-2693\(01\)00362-8](https://doi.org/10.1016/S0370-2693(01)00362-8) (cited on page 9).
- [56] J. Orloff, A. N. Rozanov, and C. Santoni. "Limits on the mixing of tau neutrino to heavy neutrinos". In: *Phys. Lett. B* 550 (2002), pp. 8–15. doi: [10.1016/S0370-2693\(02\)02769-7](https://doi.org/10.1016/S0370-2693(02)02769-7) (cited on pages 10, 11).
- [57] I. Boiarska et al. "Blast from the past: constraints from the CHARM experiment on Heavy Neutral Leptons with tau mixing". In: (July 2021) (cited on pages 10, 11).
- [58] A. Cooper-Sarkar et al. "Search for heavy neutrino decays in the BEBC beam dump experiment". In: *Physics Letters B* 160.1 (1985), pp. 207–211. doi: [https://doi.org/10.1016/0370-2693\(85\)91493-5](https://doi.org/10.1016/0370-2693(85)91493-5) (cited on page 10).

- [59] B. Shuve and M. E. Peskin. "Revision of the LHCb Limit on Majorana Neutrinos". In: *Phys. Rev. D* 94.11 (2016), p. 113007. doi: [10.1103/PhysRevD.94.113007](https://doi.org/10.1103/PhysRevD.94.113007) (cited on page 10).
- [60] R. Aaij et al. "Search for heavy neutral leptons in  $W^+ \rightarrow \mu^+ \mu^\pm$ jet decays". In: *Eur. Phys. J. C* 81.3 (2021), p. 248. doi: [10.1140/epjc/s10052-021-08973-5](https://doi.org/10.1140/epjc/s10052-021-08973-5) (cited on page 10).
- [61] R. Plestid. "Luminous solar neutrinos I: Dipole portals". In: *Phys. Rev. D* 104 (2021), p. 075027. doi: [10.1103/PhysRevD.104.075027](https://doi.org/10.1103/PhysRevD.104.075027) (cited on pages 11, 12).
- [62] A. Osipowicz et al. "KATRIN: A Next generation tritium beta decay experiment with sub-eV sensitivity for the electron neutrino mass. Letter of intent". In: (Sept. 2001) (cited on page 11).
- [63] S. Mertens et al. "A novel detector system for KATRIN to search for keV-scale sterile neutrinos". In: *Journal of Physics G: Nuclear and Particle Physics* 46.6 (2019), p. 065203. doi: [10.1088/1361-6471/ab12fe](https://doi.org/10.1088/1361-6471/ab12fe) (cited on page 11).
- [64] M. Aker et al. "Search for keV-scale sterile neutrinos with the first KATRIN data". In: *Eur. Phys. J. C* 83.8 (2023), p. 763. doi: [10.1140/epjc/s10052-023-11818-y](https://doi.org/10.1140/epjc/s10052-023-11818-y) (cited on page 11).
- [65] B. Abi et al. "Deep Underground Neutrino Experiment (DUNE), Far Detector Technical Design Report, Volume II: DUNE Physics". In: (Feb. 2020) (cited on page 11).
- [66] S. Friedrich et al. "Limits on the Existence of sub-MeV Sterile Neutrinos from the Decay of  ${}^7\text{Be}$  in Superconducting Quantum Sensors". In: *Phys. Rev. Lett.* 126.2 (2021), p. 021803. doi: [10.1103/PhysRevLett.126.021803](https://doi.org/10.1103/PhysRevLett.126.021803) (cited on page 11).
- [67] C. Hagner et al. "Experimental search for the neutrino decay  $\nu_3 + \nu_j + e^+ + e^-$  and limits on neutrino mixing". English. In: 52.3 (1995), pp. 1343–1352. doi: [10.1103/PhysRevD.52.1343](https://doi.org/10.1103/PhysRevD.52.1343) (cited on page 11).
- [68] R. Plestid. "Luminous solar neutrinos II: Mass-mixing portals". In: *Phys. Rev. D* 104 (2021). [Erratum: *Phys. Rev. D* 105, 099901 (2022)], p. 075028. doi: [10.1103/PhysRevD.104.075028](https://doi.org/10.1103/PhysRevD.104.075028) (cited on page 12).
- [69] P. Coloma et al. "Double-Cascade Events from New Physics in Icecube". In: *Phys. Rev. Lett.* 119.20 (2017), p. 201804. doi: [10.1103/PhysRevLett.119.201804](https://doi.org/10.1103/PhysRevLett.119.201804) (cited on page 12).
- [70] P. Coloma. "Icecube/DeepCore tests for novel explanations of the MiniBooNE anomaly". In: *Eur. Phys. J. C* 79.9 (2019), p. 748. doi: [10.1140/epjc/s10052-019-7256-8](https://doi.org/10.1140/epjc/s10052-019-7256-8) (cited on page 12).
- [71] M. Atkinson et al. "Heavy Neutrino Searches through Double-Bang Events at Super-Kamiokande, DUNE, and Hyper-Kamiokande". In: *JHEP* 04 (2022), p. 174. doi: [10.1007/JHEP04\(2022\)174](https://doi.org/10.1007/JHEP04(2022)174) (cited on page 12).
- [72] P. Coloma et al. "GeV-scale neutrinos: interactions with mesons and DUNE sensitivity". In: *Eur. Phys. J. C* 81.1 (2021), p. 78. doi: [10.1140/epjc/s10052-021-08861-y](https://doi.org/10.1140/epjc/s10052-021-08861-y) (cited on pages 12, 18).
- [73] M. Tanabashi et al. "Review of Particle Physics". In: *Phys. Rev. D* 98 (3 Aug. 2018), p. 030001. doi: [10.1103/PhysRevD.98.030001](https://doi.org/10.1103/PhysRevD.98.030001) (cited on pages 13, 15).
- [74] M. Honda et al. "Atmospheric neutrino flux calculation using the NRLMSISE-00 atmospheric model". In: *Phys. Rev. D* 92 (2 July 2015), p. 023004. doi: [10.1103/PhysRevD.92.023004](https://doi.org/10.1103/PhysRevD.92.023004) (cited on pages 13, 26).
- [75] A. Fedynitch et al. "Calculation of conventional and prompt lepton fluxes at very high energy". In: *European Physical Journal Web of Conferences*. Vol. 99. European Physical Journal Web of Conferences. Aug. 2015, p. 08001. doi: [10.1051/epjconf/20159908001](https://doi.org/10.1051/epjconf/20159908001) (cited on page 14).
- [76] P. A. M. Dirac. "The Quantum Theory of the Emission and Absorption of Radiation". In: *Proceedings of the Royal Society of London Series A* 114.767 (Mar. 1927), pp. 243–265. doi: [10.1098/rspa.1927.0039](https://doi.org/10.1098/rspa.1927.0039) (cited on page 14).
- [77] I. Esteban et al. "The fate of hints: updated global analysis of three-flavor neutrino oscillations". In: *JHEP* 09 (2020), p. 178. doi: [10.1007/JHEP09\(2020\)178](https://doi.org/10.1007/JHEP09(2020)178) (cited on page 15).
- [78] A. Terliuk. "Measurement of atmospheric neutrino oscillations and search for sterile neutrino mixing with IceCube DeepCore". PhD thesis. Berlin, Germany: Humboldt-Universität zu Berlin, Mathematisch-Naturwissenschaftliche Fakultät, 2018. doi: [10.18452/19304](https://doi.org/10.18452/19304) (cited on page 16).
- [79] J. A. Formaggio and G. P. Zeller. "From eV to EeV: Neutrino cross sections across energy scales". In: *Rev. Mod. Phys.* 84 (3 Sept. 2012), pp. 1307–1341. doi: [10.1103/RevModPhys.84.1307](https://doi.org/10.1103/RevModPhys.84.1307) (cited on page 17).

- [80] V. Barger et al. "Matter effects on three-neutrino oscillations". In: *Phys. Rev. D* 22 (11 Dec. 1980), pp. 2718–2726. doi: [10.1103/PhysRevD.22.2718](https://doi.org/10.1103/PhysRevD.22.2718) (cited on page 21).
- [81] A. M. Dziewonski and D. L. Anderson. "Preliminary reference Earth model". In: *Physics of the Earth and Planetary Interiors* 25.4 (1981), pp. 297–356. doi: [https://doi.org/10.1016/0031-9201\(81\)90046-7](https://doi.org/10.1016/0031-9201(81)90046-7) (cited on page 21).
- [82] S. Yu and J. Micallef. "Recent neutrino oscillation result with the IceCube experiment". In: *38th International Cosmic Ray Conference*. July 2023 (cited on pages 22, 27).
- [83] L. Fischer, R. Naab, and A. Trettin. "Treating detector systematics via a likelihood free inference method". In: *Journal of Instrumentation* 18.10 (2023), P10019. doi: [10.1088/1748-0221/18/10/P10019](https://doi.org/10.1088/1748-0221/18/10/P10019) (cited on page 25).
- [84] E. Lohfink. "Testing nonstandard neutrino interaction parameters with IceCube-DeepCore". PhD thesis. Mainz, Germany: Johannes Gutenberg-Universität Mainz, Fachbereich für Physik, Mathematik und Informatik, 2023. doi: <http://doi.org/10.25358/openscience-9288> (cited on page 25).
- [85] J. Evans et al. "Uncertainties in atmospheric muon-neutrino fluxes arising from cosmic-ray primaries". In: *Phys. Rev. D* 95 (2 Jan. 2017), p. 023012. doi: [10.1103/PhysRevD.95.023012](https://doi.org/10.1103/PhysRevD.95.023012) (cited on page 27).
- [86] G. D. Barr et al. "Uncertainties in Atmospheric Neutrino Fluxes". In: *Phys. Rev. D* 74 (2006), p. 094009. doi: [10.1103/PhysRevD.74.094009](https://doi.org/10.1103/PhysRevD.74.094009) (cited on page 27).
- [87] J. Feintzeig. "Searches for Point-like Sources of Astrophysical Neutrinos with the IceCube Neutrino Observatory". PhD thesis. University of Wisconsin, Madison, Jan. 2014 (cited on page 27).
- [88] N. Kulacz. "In Situ Measurement of the IceCube DOM Efficiency Factor Using Atmospheric Minimum Ionizing Muons". MA thesis. University of Alberta, 2019 (cited on page 27).
- [89] M. G. Aartsen et al. "Computational techniques for the analysis of small signals in high-statistics neutrino oscillation experiments". In: *Nucl. Instrum. Meth. A* 977 (2020), p. 164332. doi: [10.1016/j.nima.2020.164332](https://doi.org/10.1016/j.nima.2020.164332) (cited on page 27).
- [90] <https://github.com/icecube/pisa> (cited on page 27).
- [91] R. S. Nickerson. "Confirmation Bias: A Ubiquitous Phenomenon in Many Guises". In: *Review of General Psychology* 2 (1998), pp. 175–220 (cited on page 27).
- [92] H. Dembinski et al. *scikit-hep/iminuit: v2.17.0*. Version v2.17.0. Sept. 2022. doi: [10.5281/zenodo.7115916](https://doi.org/10.5281/zenodo.7115916) (cited on page 28).
- [93] F. James and M. Roos. "Minuit: A System for Function Minimization and Analysis of the Parameter Errors and Correlations". In: *Comput. Phys. Commun.* 10 (1975), pp. 343–367. doi: [10.1016/0010-4655\(75\)90039-9](https://doi.org/10.1016/0010-4655(75)90039-9) (cited on page 28).
- [94] S. S. Wilks. "The Large-Sample Distribution of the Likelihood Ratio for Testing Composite Hypotheses". In: *The Annals of Mathematical Statistics* 9.1 (1938), pp. 60–62. doi: [10.1214/aoms/1177732360](https://doi.org/10.1214/aoms/1177732360) (cited on page 30).